Cloud history can change water-ice-surface interactions of oxide mineral aerosols: a case study on silica

Ahmed Abdelmonem[1*], Sanduni Ratnayake[2], Jonathan D. Toner[3] and Johannes Lützenkirchen[2]

[1]Institute of Meteorology and Climate Research - Atmospheric Aerosol Research (IMKAAF), Karlsruhe Institute of Technology (KIT), 76344 Eggenstein-Leopoldshafen, Germany
[2]Institute of Nuclear Waste Disposal (INE), Karlsruhe Institute of Technology (KIT), 76344 Eggenstein-Leopoldshafen, Germany
[3]Department of Earth & Space Sciences, University of Washington, Seattle, WA 98195, USA
* Correspondence to: A. Abdelmonem (ahmed.abdelmonem@kit.edu)

***Correspondence to*: Ahmed Abdelmonem (ahmed.abdelmonem@kit.edu)**

Final Rebuttal

ACPD

I. Point-to-point response to Reviewer 1

II. Point-to-point response to Reviewer 2

III. Revised manuscript with tracked changes

IV. Revised SI with tracked changes

Message from the Authors:

The authors would like to thank the referees for their time reading the manuscript and placing the comments and suggestions. We believe that considering the points suggested by the Referees has improved the manuscript significantly. In addition we have improved the presentation quality.

I. Point-to-point response to Referee 1 (RC1)

RC1: 1)

The manuscript submitted by Abdelmonem et al. examines the effects of freeze-melt processes on the aqueous chemistry at silica surfaces at low pH. The experiments were performed in an environmental cell in conjunction with second-harmonic generation spectroscopy. Abdelmonem et al. found a water ordering-cooling dependence that improved continuously and they proposed that water ordering is a result of the dissolution of the silica surface and that this process causes the improved ice nucleation of aged silica samples. The manuscript is interesting but focused mostly on SHG measurements. Therefore it seems more relevant for a more physical chemical journal and in the current form the conclusions of the SHG measurements and their relevance and connection for atmospheric research are not evident.

AC1:1)

The authors generally agree with the opinion of the Reviewer, but would like to clarify important points:

SHG has only been used here as a technique to examine the water structure at the surface. The authors didn't add novelty in SHG theory or discuss its details. ACP has published many articles on ice nucleation and interactions in atmosphere using ESM, AFM, IR-spectroscopy …etc. All these articles were considered atmosphere relevant based on the aim of the study irrespective of the technique. Indeed, the application of SHG and SFG in atmospheric science is something new and beneficial for atmospheric science and the respective journals to consider new techniques.

This work has been triggered by the wide scatter of experimental results on ice nucleation abilities of atmospheric aerosol particles, as has been well demonstrated by (Hoose and Mohler, 2012) in their ACP review of results from six decades of laboratory experiments of heterogeneous ice nucleation. Hoose and Mohler concluded with the recommendation of performing experiments (spectroscopic, microscopic and chemical characterization methods) with pure and homogeneous materials to improve the understanding of the basic physical and chemical principles of heterogeneous ice nucleation. This manuscript discusses the influence of surface aging on heterogeneous freezing, a crucial process in cloud formation. Therefore the authors believe that the Journal of "Atmospheric Chemistry and Physics" is the most relevant.

RC1: 2)

SHG probes the average of the ensemble of all water molecules underneath the heterogeneous silica sample. Yet, ice nucleation on α-quartz surfaces was shown to occur at only a few locations which were associated with micron-size surface pits. (Holden et al. 2019 Science Advances). The authors should include this important point into the manuscript so that the readers can better put the SHG results in perspective. The authors should also think about possible topographical changes on the silica due to pH 3 treatment as this might also be able to explain the improved ice nucleation. The authors might also want to consider providing evidence whether their silica substrates become better ice nucleators with time.

AC1:2)

The authors would like to point that the sample is not heterogeneous but rather a homogeneous polished fused silica sample. This manuscript doesn't touch on active sites, rather the role of surface interactions in enhancing or resisting the ice formation. Our sample is fused silica which is not identical to α-quartz. Nevertheless, the authors have cited the work suggested by the Reviewer as it demonstrates the difficulty of predicting and controlling crystal formation.

The authors couldn't detect any topographical changes on the silica due to pH 3 treatment. AFM measurements yielded no results that would support such change. Figure (AC1.1) shows a comparison between (1) cleaned sample and (b) sample after experiment. The authors did not rely on these results as a proof that the topography has not been changed because the AFM measurements were done off-line and hitting the exact spot where SHG was measuring was not guaranteed.

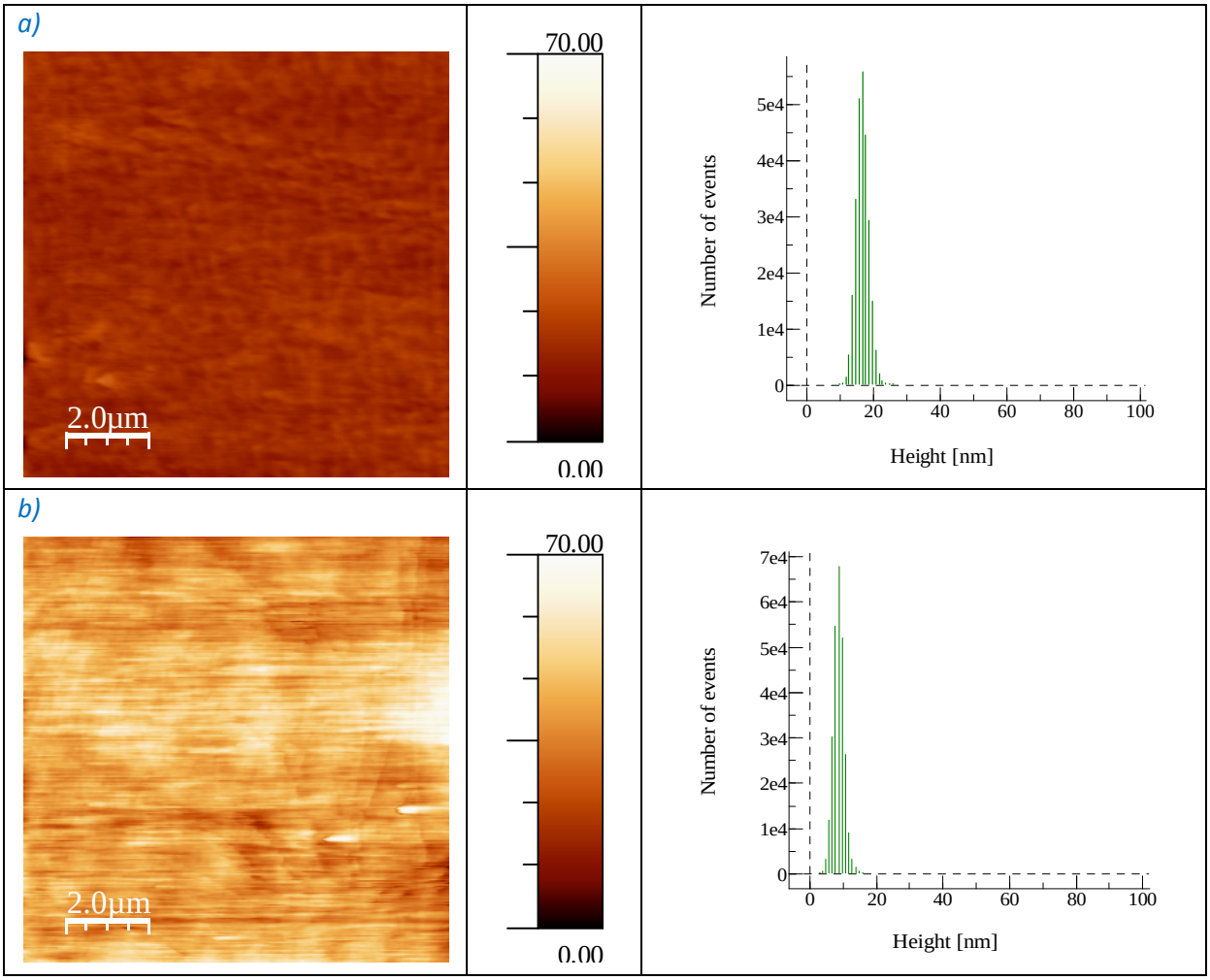

Figure (AC1.1): AFM measurements on the surface of the silica sample after cleaning (a) and after freezing-melting experiments (b).

We see the increase in the freezing temperature under identical conditions as a function of aging, Figure (5) in the manuscript. High statistics freezing assay could provide second evidence that silica substrates become better ice nucleators, but it was not available during this study.

Introduction:

RC1: 3)

p.3. l. 5- The discussion about the pH solubility of silica is not presented in great clarity and it is not directly clear why pH 3 is relevant for atmospheric conditions. When reading the introduction it seems that higher alkaline pH would be much more relevant.

AC1:3)

In the introduction, the high pH was only an example on the effect of droplet size change on the pH value of the cloud droplet. This is also valid for low pH. Slightly acidic or alkaline will be extreme acidic or alkaline with droplet evaporation, respectively. As mentioned in the manuscript, silica dissolution in aquatic solution is always possible however is extreme at high and very low pH as well. The choice of pH3 in the spectroscopic measurements has different reasons. As mentioned in the original manuscript p.5. l.2-3, "We chose pH = 3 because it is close to the point of zero charge of the used sample and by that we eliminate the contribution from $\chi^{(3)}$*. Also at this pH the dissolution rate is minimum as mentioned in the introduction."*

RC1: 4)

p.3 l. 42 "molecular level" this statement should be altered. In the presented experiments a large ensemble of water molecules are probed the term molecular-level might be misleading.

AC1:4)

The "molecular level" term is associated with SHG and SFG since their first results provided by Shen (Shen, 1989), as the signal allows in-situ mapping of the molecular arrangement at the surface. We only re-use the term, it is not our definition. The SHG/SFG signal depends on the "molecular hyperpolarizability tensor elements" which could allow the determination of absolute orientation of the molecules at the surface (Goh et al., 1988). We add here a selection of SHG/SFG articles which directly used the term "molecular level":

(Silva and Miranda, 2016; Gonella et al., 2016; Jerome et al., 2002; Lambrakos et al., 1998; Xiao et al., 1997; Tohda, 1996; Ashwell et al., 1992; Wang et al., 2019; Schlegel et al., 2019; Li et al., 2019; Feugmo et al., 2019; Ulrich et al., 2017; Takeshita et al., 2017; Abdelmonem et al., 2017a; Zhang et al., 2016; Wang et al., 2016; Leng et al., 2016; Luca et al., 1995).

Experimental:

RC1: 5)

p.4 l. 15 Are there any information on the surface roughness or homogeneity of your silica samples?

AC1:5)

The authors agree with the Reviewer, the surface specifications were missing in the manuscript. The surface of the silica samples is optically polished, surface quality is 40-20 Scratch-Dig and surface flatness at 633 nm is Lambda/10. This information has been added to the experimental section in the revised manuscript (p. 4,l. 10-11).

RC1: 6)

p.4. l. 34 “the incident angle was adjusted to 1 degree above the critical anlge of TIR to guarantee a TIR condition in the studied temperature range. Why was +1 degree chosen and why would the incident angle change? Which effect would the changing angle of incident have on your data?

AC1:6)

The issue is more about the change in the critical angle and not the incident angle. The critical angle for TIR at the silica/water interface is a function of the refractive indices of both silica and water. It is well known that the refractive index is temperature and phase-of-matter dependent. We fix the incident angle, but the critical angle may cross the incident angle during cooling and freezing and then violates the TIR condition. Violation of the TIR condition will result in a clear drop in the signal and make data interpretation difficult. Any incident angle higher than the range of changes in the critical angle with temperature should be acceptable. Figure (AC1.2) shows the change in the refractive indices of water and ice and the critical angle with temperature in the temperature range of our experiments. Simple calculations based on Snell's law show that the change in the critical angle for the water/silica system in the studied temperature range (red triangles) is less than 0.5°. We used an incident angle = critical angle + 1°, however any higher angle would also be fine regarding the TIR condition.

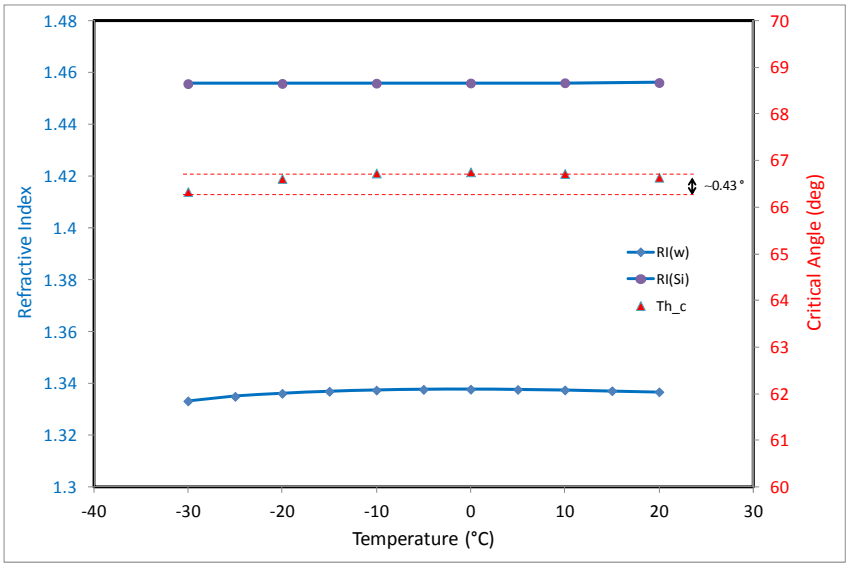

Figure AC1.2: The change in the Refractive index and the corresponding change in critical angle of TIR as a function of temperature for Si/water interface. The temperature dependent refractive indices are taken from (Cho et al., 2001; Waxler and Cleek, 1971)

RC1: 7)

p.4 l. 35 Were the Fresnel factors corrected for the effect of temperature? Does it affect the silica measurements?

AC1:7)

We did not correct the data in Figure (4) for the effect of temperature. The effect of temperature on Fresnel factors in the range of temperatures studied here is small for the water/silica interface, (red crosses, Figure AC1.3). However this is not the reason to ignore them. As each panel in Figure 4 shows the change in SHG with aging at constant temperature, correction to Fresnel factors has no effect and this is the reason why data in Fig(4) are not Fresnel corrected.

Only the discussion on the transient signal, Figure 7, required Fresnel factors correction, for two reasons: 1) Data are compared at both different temperatures and different phase-of-matter (liquid and ice). 2) There is a significant difference between Fresnel factors of liquid and ice as can be seen in Figure AC1.3 (red crosses and blue X respectively).

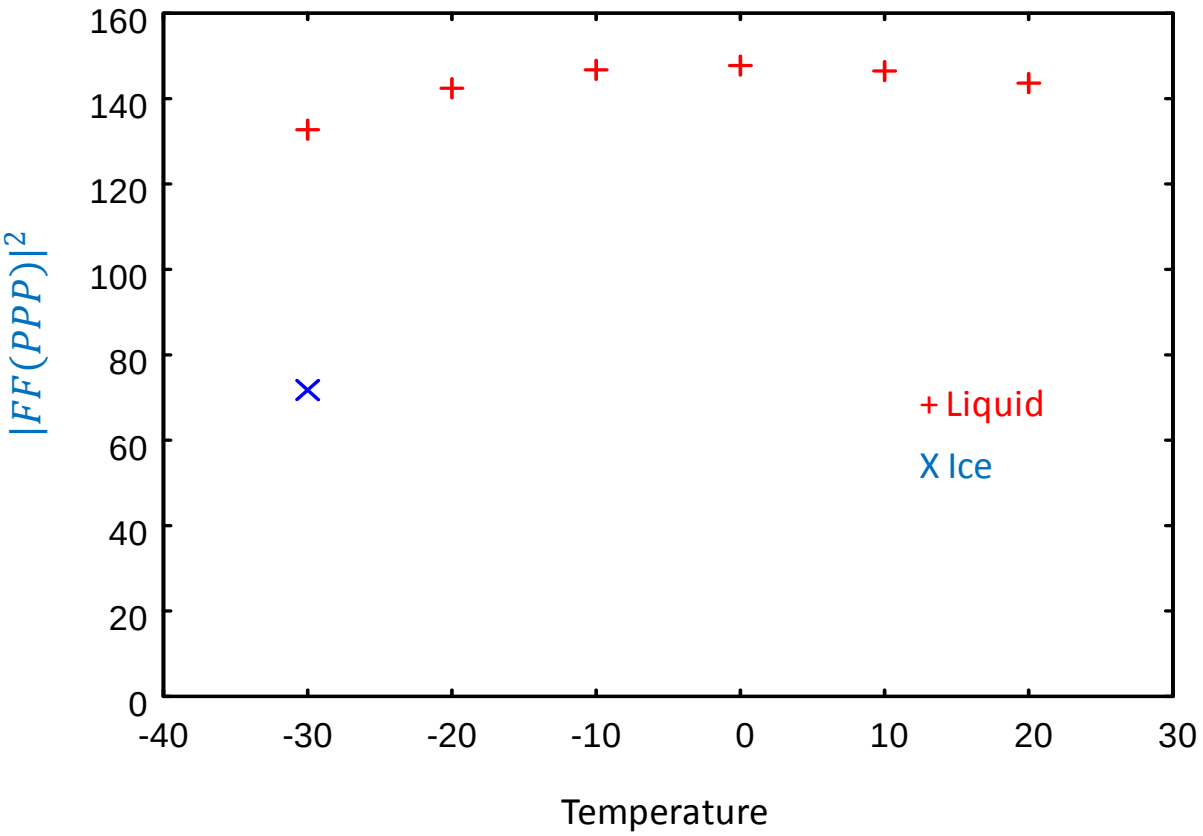

Figure AC1.3: The change in the Fresnel factors as a function of temperature for silica/water interface (red crosses) and the value for Si/ice interface (blue X).

RC1: 8)

Does the volume stay the same during the longer successive runs and are evaporation effects possible/considered?

AC1:8)

As mentioned in the Experimental section, the measuring cell is tightly closed and sealed during the measurements. Volume changes are not expected.

RC1: 9)

p. 6 Fig. 2: The light grey scan and the turquoise scan were cut after 1500 s without an explanation. Full data sets should be shown.

AC1:9)

We thank the Reviewer for this remark. We have included a comment on this deficiency in the figure caption in the revised version. Sometimes, due technical reasons, the data acquisition software crashes and some data points are missing, (e.g. the light grey (cycle 2) and the turquoise (cycle 16) scans). The lost data in these two scans are in the end of the scan where, as can be seen from the other 23 scans, no exceptional change is expected. Omitting cycles 2 and 16 from the presented data set wouldn't affect our interpretations. However, we wanted to present all collected scans with constant interval between them.

RC1: 10)

p.8 Fig.4: Fig4b and c seem identical. It would be much more convincing if they would add a point at 2000 s to see how this signal changes as a function of cycles. From the data presented in Figure 2 it seems that except for Run 1 the intensities look comparable.

AC1:10)

Indeed Fig 4c seems identical to 4b. However, it is our intention to show that at the onset point, Fig 4c, nothing exceptional happens although the onset temperatures are different. Nevertheless it is a good point to show the change in signal with aging at other temperatures. Since the paper discusses the restructuring of water upon cooling and relates this to the freezing process, data at 2000 s may not be the right choice. At time 2000 s there is liquid signal after partial melting with undefined amounts of melted ice and solute concentration. What could be useful to compare after melting is the liquid signal at room temperature after each complete freeze-melt cycle. But this is already included in panel a (e.g. the room temperature liquid signal after first scan is the room temperature liquid signal of the second cycle).

We select here a set of temperatures during cooling to plot the liquid signal as a function of cycle number. Figure AC1.4 shows the averaged SHG liquid signal as a function of TP cycle number at five different temperatures on the cooling path. The minimum points occur at lower cycle numbers for lower temperatures (summarized in table AC1.1). This supports our conclusion that cooling favors the uptake of dissolved silica (i.e. adsorption).

Time with respect to scan start (s)	Temperature (°C)	Closest cycle no. to minimum signal
a) 0 sec	20	7
b) 120 sec	10	6
c) 240 sec	0	5
d) 480 sec	-20	4
e) 630 sec	-32	3

Table AC1.1: The selected temperatures in Figure AC1.4 and the closest TP cycle number of minimum SHG liquid signal.

Figure AC1.4 and Table AC1.1 have been included in the supporting information and the corresponding discussion has been changed in the revised manuscript.

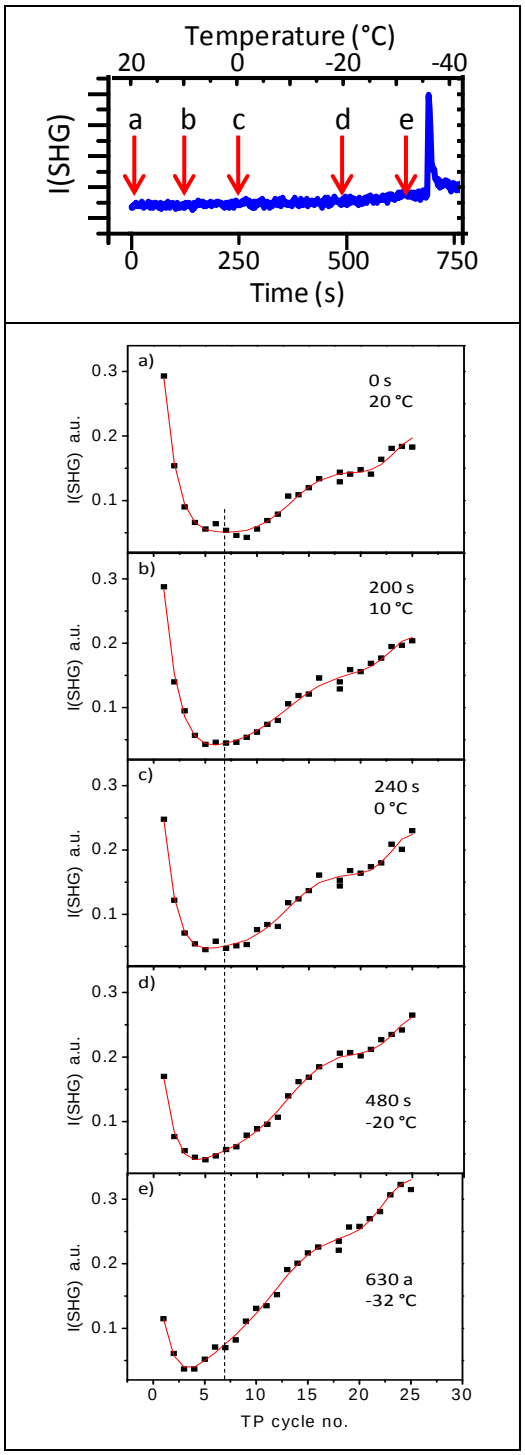

Figure AC1.4: Upper panel: a sample plot of SHG vs. time/temperature during cooling. Lower panel: The averaged SHG liquid signal as a function of TP cycle number at five different temperatures during cooling before freezing. The red lines on the plots are guiding lines through the data points.

RC1: 11)

p.8 Fig. 4 Are there any indications from your data that the onset of the freezing occurs at earlier timings when the samples are aged?

AC1:11)

Yes this is directly indicated by Figure 5.

RC1: 12)

p.9 l. 1-5 Control experiments at lower temperature, not RT would be helpful since the pH depends on the temperature.

AC1:12)

The control experiments included the full temperature range. Comparing lower temperature shows the same result: i.e. "Pausing the freeze-melt cycles for 5 hours has minimal effect on the SHG signal in time", as can be seen in Figure AC1.5. We have replaced Figure S3 by Figure AC1.5 (now S4 in the revised version). The paragraph p. 9, l.1-8 has been changed correspondingly. Please note that comparing time axis in case of C27 is only possible at RT (20 °C) because C27 has different cooling rate as described in the manuscript.

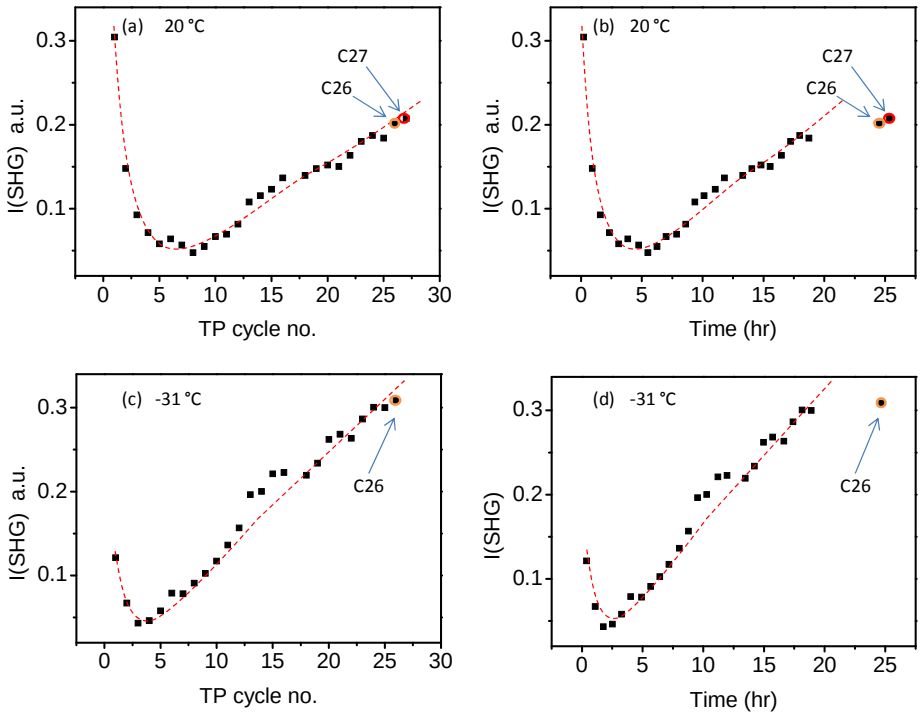

Figure AC1.5: SHG signal at pH3 solution-silica interface as a function of TP cycle number (a and c) and time (b and d) of liquid signal at 20 °C (a and b) and -31 °C (c and d) during repeating the freeze-melt TP. The dashed red lines are trend lines illustrating the behavior of the signal. For low temperature (-31 °C), only data point C26 is plotted because C27 has a different cooling rate as described in the manuscript. CS26 and CS27 lay on the trend line with plot against TP cycle number (a and c) but not with time (b and c). This shows that the significant aging we observe in this work arises from the freeze-melt process and not from the time the sample is in contact with solution.

RC1: 13)

p.9 l. 41 The statement “the older the sample” is somewhat ambiguous. Were the experiments performed on multiple independent samples? Or one silica prism and the age of the sample refers to the number of cycles the sample was exposed to. The number of used silica samples and the number of independent experiments should be added to the materials section.

AC1:13)

We thank the reviewer for pointing to this misleading term. For consistency, the data reported in this work were all collected on the same silica prism. This statement has been added to the Experimental section in the revised version (p.4, l. 10-11).

The age of the sample refers to the number of cycles the sample was exposed to. The statement “the older the sample…” has been corrected in the revised version to “the older the surface, i.e. the more often exposed to freeze-melt cycles, the higher the degree of …” (p.9, l. 42)

RC1: 14)

p.10 l. 8 What is the experimental evidence that the prism that orders water better is also a better ice nucleator? Were any experiments performed? Couldn’t the ageing process and the contact with acid also just roughen the surface and that is the reason why it nucleates better?

AC1:14)

This is a good question and we have clarified this point in the revised version (p. 10, l. 2-4).

The experimental evidence that a surface that orders water better “could be” a better ice nucleator has been recently reported (Abdelmonem et al., 2017b; Abdelmonem et al., 2015; Yang et al., 2011). Other parameters, e.g. roughness, porosity, steps…, are not excluded. We believe that all surface properties influence the ice nucleation ability though with different weights. We also believe that the way these properties influence the interaction with water molecules at the surface is the key to the overall effect. In our previous work (Abdelmonem et al., 2017a) we combined freezing assays and SFG characterizations to study the effect of surface charge on the heterogeneous ice-nucleation ability of a-alumina (0001) surfaces. We are not generalizing our former observation on that particular surface (i.e. the a-alumina (0001)), but only recall an existence of evidence.

That “Water ordering leads to better ice nucleation condition” is not that straight forward. When a surface is able to create an ordering compatible with the structure of a crystalline phase, it will then promote the nucleation of the corresponding phase particularly if the induced ordering further matches the crystalline structure at a higher degree (Bi et al., 2017). A surface may exhibit the ordering patterns that resemble the structure of ice. Therefore, water layers bound to surfaces may be ice-like, providing a template for ice to nucleate (Bi et al., 2016). Based on these facts we suggest that the re-adsorbed dissolution products have an arrangement on its surface as close as possible to that of water molecules in some low index plane of ice.

There is a lack in the literature on what happens at the surface on the molecular level and our approach is applied in ice nucleation studies only since few years ago. With this work we try to attract the attention of theoreticians who can simulate this re-adsorption of dissolution products and their arrangement on the surface. Indeed we have proposed MD simulations with the group of Molecular Modelling and Computer Simulations, Clemson University, as future cooperation.

RC1: 15)

p.10 Fig.5 Since the observed effect is not very pronounced. It would be good toadd error bars in the Figure or provide information on how reproducible the trend is.

AC1:15)

The authors agree with the Reviewer, this information was missing in the figure caption. Repeating the experiment showed the same trend over the whole range of cycles with an average standard deviation of 1.3. The information has been added in the figure caption with the corresponding error bars on Figure 5 in the revised version of the manuscript.

RC1: 16)

p.11 l. 15 The results of the following study should be added to the discussion. Rehl et al. 2019 New Insights into χ(3) Measurements: Comparing Nonresonant Second Harmonic Generation and Resonant Sum Frequency Generation at the Silica/Aqueous Electrolyte Interface, JPCA.

AC1:16)

The study of Rehl et al. 2019, although interesting, is not relevant to our study. Rehl et al. compare the SHG and SFG from technical point of view. Neither the sample (IR-grade Silica) nor the solution (0.5 M NaCl) are the same as ours. Even the temperature effect was not discussed. They wanted to find the origin of inconsistencies between SHG and SFG that have arisen when comparing experiments on silica at high electrolyte concentrations. Discussing their results in our manuscript will confuse the reader and deviate from the main study.

However, this paper includes one very useful information which is "SHG is more sensitive to the number density of aligned water, particularly at low pH and ionic strength". As already mentioned in the first paragraph in the "Results and Discussion" section, we eliminate the $\chi^{(3)}$ effect by choosing pH = 3, and we also add no salts. We have cited this paper in this context in the revised manuscript (p. 4, l. 26-27).

RC1: 17)

p.13 l. 33 Is there an explanation why the ice signal shows such strong variations.

AC1:17)

So far we have no explanation for the strong fluctuation in the ice signal after freezing. This will need further investigations on the ice structure after freezing. One expected scenario is the formation of free OH group after freezing (as we observed on Sapphire 110 surface using SFG, not published yet). The role of the formation of this free OH is not yet known. We added the following sentence to p.13. l. 35-36: "This ice signal fluctuation merits further investigations particularly using SFG which gives details on the individual contributions of different interfacial species from their resonant vibrations.". We also merged the "Ice signal" and "Confined liquid signal" sessions.

RC1: 18)

p. 13. l. 35 Is it possible to estimate the thickness of the liquid film? I would assume this could provide very useful information as one could estimate the pH of this solution which should be much lower due to the freeze concentration and likely dissolves the silica even faster.

AC1:18)

Not with this technique. The maximum penetration depth in our geometry is ~ 400 nm. The layer thickness exceeds this distance very shortly after the freezing point (= transient peak time).

RC1: 19)

p. 14 l. 28 "this study is expected to benefit"… The connection of the results of the current study and its implications for atmospheric research are not clear.

AC1:19)

The authors have answered on this question in AC1 (second paragraph)

II. Point-to-point response to Referee 2 (RC2)

RC2: 1)

In Fig. 2, 3, and 7, it could be more intuitive to use the temperature as the x axis, instead of the time.

AC2: 1)

The authors would like to thank the Reviewer for his practical suggestion. Indeed plotting the data as a function of temperature will be more perceptive. However, this is only possible in the range of scan where the independent parameter (temperature in this case) is single-valued, otherwise the plot will be confusing, e.g. Fig. AC2.1.

Since we focus in this manuscript on the water restructuring upon cooling, plotting the SHG liquid signal as a function of temperature during cooling is the correct choice. Since Figure 3 is a subset of Figure 2, we have only replaced Figure 3 with a new one that now includes temperature as the x axis (Figure AC2.2).

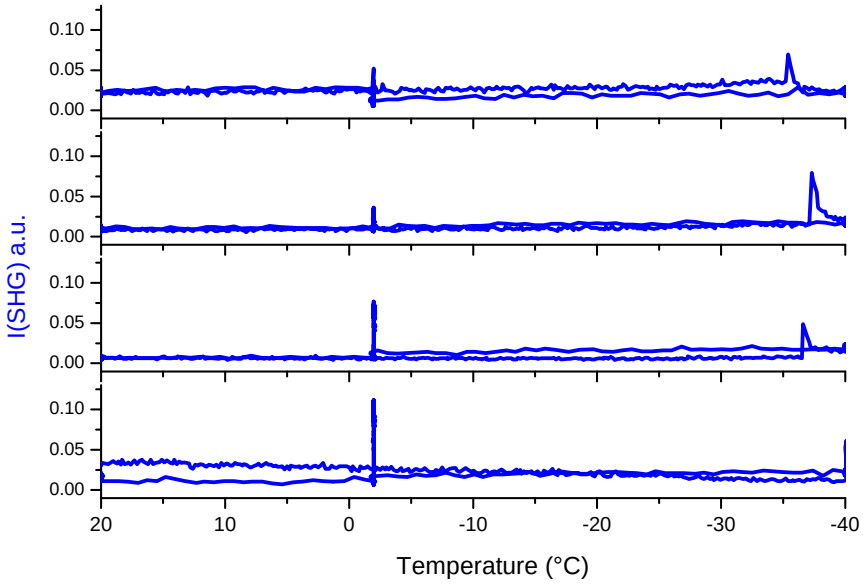

Figure AC2.1: This figure shows haw Figure 3 would look like if we plot the SHG signal of the complete scans with temperature is the x-axis.

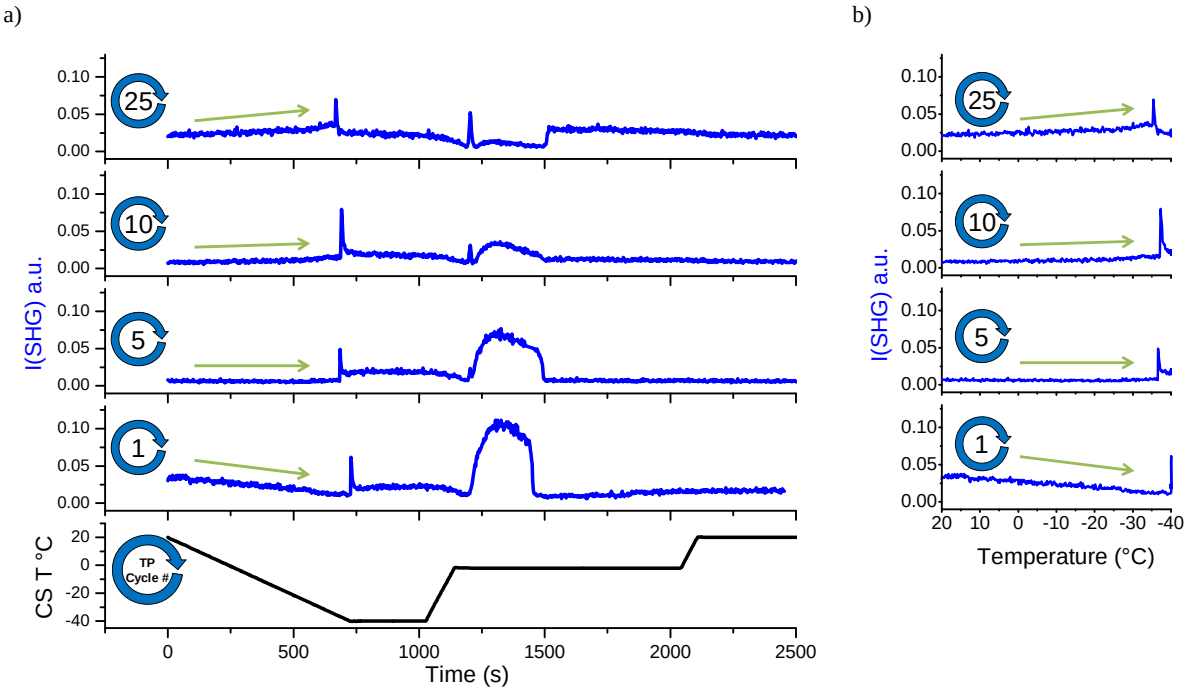

Figure AC2.2: SHG liquid signal as a function of time and temperature during cooling. Figure 3 in the manuscript has been replaced with this Figure.

Figure 7 cannot be plotted using temperature as the x axis because the temperature around the freezing and melting peaks is almost constant (i.e. again a not single-valued relation).

RC2: 2)

The data presented in the manuscript may not directly related to “cloud history”, as indicated by the title.

AC2: 2)

As mentioned in the abstract and introduction, an aerosol-containing cloud droplet can go through different freeze-melt or evaporation-condensation cycles, so that not only the aerosol surface structure may change, but also ionic strength and pH of the cloud droplet. We conclude that the cloud history may affect the contained aerosol particles. During cloud formation, water vapor condenses on aerosol particles forming liquid suspended water droplets in about a 100% RH environment. Cloud droplets are constantly forming and dissipating. Depending on the atmospheric conditions (e.g. temperature, RH, or air draft) the cloud droplet change its size. In case of temperature increase, cloud mixing with drier air, or air sinking within the cloud, cloud droplets may evaporate (may also totally dissipate). Under these conditions the acidic, basic components or ionic strength in the cloud droplet will reach extreme values. We show in this manuscript that this may significantly change the surface properties of mineral oxide aerosols. However, we agree with the Reviewer that the title of the original manuscript could be improved. The manuscript title has been changed to “Cloud history can change water-ice-surface interactions of oxide mineral aerosols: a case study on silica”.

References:

Abdelmonem, A., Lützenkirchen, J., and Leisner, T.: Probing Ice-Nucleation Processes on the Molecular Level using Second Harmonic Generation Spectroscopy, Atmos. Meas. Tech., 8, 3519-3526, doi: 10.5194/amt-8-3519-2015, 2015.

Abdelmonem, A., Backus, E. H. G., Hoffmann, N., Sanchez, M. A., Cyran, J. D., Kiselev, A., and Bonn, M.: Surface-charge-induced orientation of interfacial water suppresses heterogeneous ice nucleation on alpha-alumina (0001), Atmospheric Chemistry and Physics, 17, 7827-7837, doi: 10.5194/acp-17-7827-2017, 2017a.

Abdelmonem, A., Backus, E. H. G., Hoffmann, N., Sánchez, M. A., Cyran, J. D., Kiselev, A., and Bonn, M.: Surface-Charge-Induced Orientation of Interfacial Water Suppresses Heterogeneous Ice Nucleation on α-Alumina (0001), Atmos. Chem. Phys., 17, 7827-7837, doi: 10.5194/acp-17-7827-2017, 2017b.

Ashwell, G. J., Hargreaves, R. C., Baldwin, C. E., Bahra, G. S., and Brown, C. R.: IMPROVED 2ND-HARMONIC GENERATION FROM LANGMUIR-BLODGETT-FILMS OF HEMICYANINE DYES, Nature, 357, 393-395, doi: 10.1038/357393a0, 1992.

Bi, Y., Cabriolu, R., and Li, T.: Heterogeneous Ice Nucleation Controlled by the Coupling of Surface Crystallinity and Surface Hydrophilicity, The Journal of Physical Chemistry C, 120, 1507-1514, doi: 10.1021/acs.jpcc.5b09740, 2016.

Bi, Y., Cao, B., and Li, T.: Enhanced heterogeneous ice nucleation by special surface geometry, Nature Communications, 8, 15372, doi: 10.1038/ncomms15372, 2017.

Cho, C. H., Urquidi, J., Gellene, G. I., and Robinson, G. W.: Mixture model description of the T-, P dependence of the refractive index of water, The Journal of Chemical Physics, 114, 3157-3162, doi: 10.1063/1.1331571, 2001.

Feugmo, C. G. T., Liegeois, V., Caudano, Y., Cecchet, F., and Champagne, B.: Probing alkylsilane molecular structure on amorphous silica surfaces by sum frequency generation vibrational spectroscopy: First-principles calculations, Journal of Chemical Physics, 150, doi: 074703

10.1063/1.5080007, 2019.

Goh, M. C., Hicks, J. M., Kemnitz, K., Pinto, G. R., Heinz, T. F., Eisenthal, K. B., and Bhattacharyya, K.: Absolute orientation of water molecules at the neat water surface, J. Phys. Chem., 92, 5074-5075, doi: 10.1021/j100329a003, 1988.

Gonella, G., Lutgebaucks, C., de Beer, A. G. F., and Roke, S.: Second Harmonic and Sum-Frequency Generation from Aqueous Interfaces Is Modulated by Interference, Journal of Physical Chemistry C, 120, 9165-9173, doi: 10.1021/acs.jpcc.5b12453, 2016.

Hoose, C. and Mohler, O.: Heterogeneous ice nucleation on atmospheric aerosols: a review of results from laboratory experiments, Atmos. Chem. Phys., 12, 9817-9854, doi: 10.5194/acp-12-9817-2012, 2012.

Jerome, B., Schuddeboom, P. C., and Meister, R.: Rotational friction at the molecular level, Europhysics Letters, 57, 389-395, doi: 10.1209/epl/i2002-00473-7, 2002.

Lambrakos, S. G., Trzaskoma-Paulette, P. P., and Triandaf, I. A.: Surface-site charge-displacement model for analysis of electromodulated optical second-harmonic response at a metal surface, Applied Spectroscopy, 52, 1240-1247, doi: 10.1366/0003702981945066, 1998.

Leng, C., Sun, S. W., Zhang, K. X., Jiang, S. Y., and Chen, Z.: Molecular level studies on interfacial hydration of zwitterionic and other antifouling polymers in situ, Acta Biomaterialia, 40, 6-15, doi: 10.1016/j.actbio.2016.02.030, 2016.

Li, X., Ma, L., and Lu, X. L.: Interfacial Molecular-level Structures of Polymers and Biomacromolecules Revealed via Sum Frequency Generation Vibrational Spectroscopy, Jove-Journal of Visualized Experiments, doi: 10.3791/59380, 2019.

Luca, A. A. T., Hebert, P., Brevet, P. F., and Girault, H. H.: Surface second-harmonic generation at air/solvent and solvent/solvent interfaces, J. Chem. Soc. Faraday Trans., 91, 1763-1768, doi: 10.1039/ft9959101763, 1995.

Schlegel, S. J., Hosseinpour, S., Gebhard, M., Devi, A., Bonn, M., and Backus, E. H. G.: How water flips at charged titanium dioxide: an SFG-study on the water-TiO2 interface, Physical Chemistry Chemical Physics, 21, 8956-8964, doi: 10.1039/c9cp01131e, 2019.

Shen, Y. R.: Surface Properties Probed by Second-Harmonic and Sum-Frequency Generation, Nature, 337, 519-525, doi: 10.1038/337519a0, 1989.

Silva, H. S. and Miranda, P. B.: Probing the Molecular Ordering and Thermal Stability of Azopolymer Layer-by-Layer Films by Second-Harmonic Generation, Langmuir, 32, 9950-9959, doi: 10.1021/acs.langmuir.6b02486, 2016.

Takeshita, N., Okuno, M., and Ishibashi, T.: Molecular conformation of DPPC phospholipid Langmuir and Langmuir-Blodgett monolayers studied by heterodyne-detected vibrational sum frequency generation spectroscopy, Physical Chemistry Chemical Physics, 19, 2060-2066, doi: 10.1039/c6cp07800a, 2017.

Tohda, K.: Studies on the mechanism of the potential generation at the surface of ion-selective liquid membranes at the molecular level, Bunseki Kagaku, 45, 641-657, 1996.

Ulrich, N. W., Li, X., Myers, J. N., Williamson, J., Lu, X. L., and Chen, Z.: Distinct Molecular Structures of Edge and Middle Positions of Plasma Treated Covered Polymer Film Surfaces Relevant in the Microelectronics Industry, Ieee Transactions on Components Packaging and Manufacturing Technology, 7, 1377-1390, doi: 10.1109/tcpmt.2017.2718562, 2017.

Wang, F., Li, X., Zhang, F. R., Liu, X. Y., Hu, P. C., Beke-Somfai, T., and Lu, X. L.: Revealing Interfacial Lipid Hydrolysis Catalyzed by Phospholipase A(1) at Molecular Level via Sum Frequency Generation Vibrational Spectroscopy and Fluorescence Microscopy, Langmuir, 35, 12831-12838, doi: 10.1021/acs.langmuir.9b02284, 2019.

Wang, M. C., Li, B. L., Chen, Z., and Lu, X. L.: Molecular-Level Structures at Poly(4-vinyl pyridine)/Acid Interfaces Probed by Nonlinear Vibrational Spectroscopy, Journal of Polymer Science Part B-Polymer Physics, 54, 848-852, doi: 10.1002/polb.23978, 2016.

Waxler, R. M. and Cleek, G. W.: Refractive indices of fused silica at low temperatures, J. Res. Natl. Inst. Stand. Technol., 75A, 279-281, doi: 10.6028/jres.075A.026, 1971.

Xiao, C. Y., Feng, J. K., Huang, X. R., Jia, Q., Sun, J. Z., Fang, Q., and Jiang, M. H.: A theoretical study on the second harmonic generation properties of molecules and crystals of 4,5-bis(2',4'-dinitrophenylthio)-1,3-dithiole-2-one(BNPT-DTO) and 4,5-bis(2',4'-dinitrophenylthio)-1,3-dithiole-2-thione(BNPT-DTT), Acta Chimica Sinica, 55, 866-871, 1997.

Yang, Z., Bertram, A. K., and Chou, K. C.: Why Do Sulfuric Acid Coatings Influence the Ice Nucleation Properties of Mineral Dust Particles in the Atmosphere?, J. Phys. Chem. Lett., 2, 1232-1236, doi: 10.1021/jz2003342, 2011.

Zhang, X. X., Myers, J. N., Huang, H., Shobha, H., Chen, Z., and Grill, A.: SFG analysis of the molecular structures at the surfaces and buried interfaces of PECVD ultralow-dielectric constant pSiCOH, Journal of Applied Physics, 119, doi: 10.1063/1.4942442, 2016.

III. Revised manuscript with tracked changes

Cloud history can change~~s~~ water-ice-surface interactions of oxide mineral aerosols ~~(e.g. Silica)~~: a case study on silica

Ahmed Abdelmonem[1*], Sanduni Ratnayake[2], Jonathan D. Toner[3] and Johannes Lützenkirchen[2]

[1]Institute of Meteorology and Climate Research - Atmospheric Aerosol Research (IMKAAF), Karlsruhe Institute of Technology (KIT), 76344 Eggenstein-Leopoldshafen, Germany
[2]Institute of Nuclear Waste Disposal (INE), Karlsruhe Institute of Technology (KIT), 76344 Eggenstein-Leopoldshafen, Germany
[3]Department of Earth & Space Sciences, University of Washington, Seattle, WA 98195, USA
* Correspondence to: A. Abdelmonem (ahmed.abdelmonem@kit.edu)

Abstract

Mineral aerosol particles ~~can act as~~nucleate ice ~~nucleators~~, and many insights have been obtained on water freezing as a function of mineral surface properties such as ~~the~~ charge or morphology. Previous studies have mainly focused on pristine samples, despite the fact that aerosol particles age under natural atmospheric conditions~~, aerosol particles age.~~. For example, an aerosol-containing cloud droplet can go through ~~different~~ freeze-melt or evaporation-condensation cycles~~, so~~ that ~~not only~~change the ~~aerosol~~ surface structure ~~may change, but also~~, the ionic strength and pH ~~of the cloud droplet. The potential variation of the~~ . Variations in the surface properties of ~~an~~ ice nucleating ~~particle during its residence~~particles in the atmosphere ~~has~~have been largely overlooked. Here, we use an environmental cell in conjunction with nonlinear spectroscopy (second-harmonic generation) to study the effect of freeze-melt processes on the aqueous chemistry at silica ~~surface~~surfaces at low pH. We found that ~~the~~ successive freeze-melt cycles disrupt the dissolution equilibrium, substantially changing the surface properties, giving rise to marked variations in the interfacial water structure and the ice nucleation ability of the surface. The degree-of-order of water molecules, next to the surface, at ~~a specific~~any temperature~~,~~ during cooling decreases and then increases again with sample aging. ~~The~~ Along the aging process, the water ordering–cooling dependence and ice nucleation ability improve continuously.

1 Introduction

Water- and ice-mineral interactions play vital roles in the atmosphere as well as in food, pharmaceutical, construction, chemical, and other industries. The chemical and morphological properties of aerosol surfaces play direct and indirect roles in the climate system. For atmospheric questions, ~~these systems should be looked up under~~in which aerosols are often in metastable, non-equilibrium ~~conditions, as in nature, atmospheric constituents are not in rest. Understanding the role of~~states, understanding how surface properties ~~and their potential variations under~~ change at different atmospheric conditions remains challenging. For example, the ice nucleation ~~(IN)~~ ability of an ice nucleating particle ~~(INP)~~ may be influenced by the change in surface properties due to aging ~~processes in ice nuclei~~ (Coluzza et al., 2017) or other secondary ice processes (Zipori et al., 2018). Solutes are able to affect freezing (Zobrist et al., 2008) ~~and as recently shown,~~ even ~~in minor concentration~~at low concentrations (Whale et al., 2018). ~~Water~~ Depending on the atmospheric conditions, water molecules may heterogeneously crystallize next to an ~~INP~~ice nucleating particle surface, forming ~~one of the~~ various ice polymorphs with different physical ~~properties depending on the atmospheric conditions (e.g. degree of supersaturation)~~ and/or surface properties (Parambil et al., 2014). This in turn affects their interaction with radiation in the atmosphere ~~for instance and has a well known impact on,~~ which impacts the energy budget of the planet (Steiner et al., 2013). In mixed phase clouds, for example, different ice polymorphs ~~of ice can~~ scatter light at different angles ~~and hence affect~~, which affects the radiation balance. Clouds and cloud formation are significant perturbations in ~~the~~ climate models ~~. This means that understanding~~ ; hence it is important to understand the elemental processes of ~~IN~~ice nucleation and the role of surface properties ~~have become a demand~~ to counteract the climate change, for example by controlling the ~~IN~~ice nucleation processes in atmosphere.

~~IN~~Ice nucleation and crystallization processes are highly dependent on the initial stages where few molecules or ions start to form a tiny crystalline nucleus in the liquid (Sosso et al., 2016; Cox et al., 2007; Cox et al., 2013). It is not possible to predict the time and place this nucleus will form in a real system. This complicates interpretations of experimental nucleation studies. Additionally, ~~a~~ pre-adsorption of small impurities on the aerosol surface can dramatically affect the ~~IN~~ice nucleation process. On the other hand, theoretical and simulation studies are complex not only because of the additional complication of describing the surface and the surface-solute interactions, but also because of potential surface modifications under atmospheric conditions. Nucleation and crystallization are very active areas of current research.

Most ~~IN~~ice nucleation processes occurring in the atmosphere are, in fact, heterogeneous, due to the omnipresence ~~INPs.~~of ice nucleating particles. Hoose and Möhler (2012) have ~~reported the wide scatter in IN efficiencies of same~~shown that ice nucleation is highly variable for aerosol particles collected from different sources and examined in different laboratories (Hoose and Mohler, 2012). There have been previous efforts to understand the influence of surface properties on water freezing, such as the effects of charge, e.g., on ice formation by aluminum oxide (Anim-Danso et al., 2016; Abdelmonem et al., 2017) or morphology, e.g., ~~for Feldspar (Kiselev et al., 2017)~~for feldspar and ~~Kaolinite~~a-quartz (Kiselev et al., 2017; Holden et al., 2019; Harrison et al., 2016) and kaolinite (Wang et al., 2016). Although predicting and controlling crystal formation is a complex problem, it is believed that ice nucleation on α-quartz only occurs at a few locations, which are associated with micron-size surface pits (Holden et al., 2019). One common effect that appears to have received relatively little attention ~~or is identified as a topic for future studies~~ (Coluzza et al., 2017) ~~–~~ is the potential variation of surface properties of a given ~~INP~~ ice nucleating particle over its residence time in the atmosphere. An aerosol particle in a cloud droplet is ~~to some extent~~ very similar to a particle in ~~a~~ solution. The ionic strength and pH of this solution may change due to different reasons. For example, an insoluble aerosol particle like silica may adsorb soluble salts like NaCl or acids like HCl or H_2SO_4 from the atmosphere or even at the surface of the earth before being aerosolized. Under suitable supersaturation conditions, water molecules in the atmosphere condense on the surface of that aerosol particle forming a ~~so called~~ cloud droplet ~~. Actually it should rather be called a~~ (we prefer term them solution droplet ~~.~~). The ionic strength ~~as well as the acid/basic character of this solution droplet is~~and pH of droplets are determined by the concentrations of all involved salts,

acids and bases~~, respectively.~~. These may affect the interfacial chemistry at the solid surface, e.g. through dissolution (Lis et al., 2014).

~~According to the literature,~~Silica dissolution ~~of silica~~ may change the ionic strength of interfacial water, which ~~may in turn change~~changes the surface charge and also ~~screen~~screens this charge by nearby ions (Seidel et al., 1997; Schaefer et al., 2017). Silica dissolution under non-equilibrium conditions, namely flow, has been recently discussed in some ~~details~~detail (Schaefer et al., 2018). They demonstrated that silica equilibrates at the interface with pure water at around 1mM ~~of~~ ionic strength~~. In~~; however, in the atmosphere, ~~the rate of~~ surface properties ~~changes, however, is~~change at variable rates depending on ~~the change in~~how the droplet size changes upon further condensation or partial evaporation. Partial evaporation may drive the system to rather extreme ~~changes of mineral INP surface properties.~~salinity and pH. A typical 50 µm mixed phase droplet of ~~a size of 50 µm with a pH value of~~ pH 8 (assuming ~~an initial~~ 1 µM NaOH solution) may evolve to pH ~~=~~ 10 when the size is reduced to its half (i.e. 25 µm~~).~~) during evaporation. At this pH ~~value~~, silica ~~for example undergoes significant dissolution with fast rates~~rapidly dissolves (Hiemstra and van Riemsdijk, 1990). ~~A possible worst case scenario could be near~~ Near complete evaporation ~~under dry conditions which~~ will drive pH and ionic strength to extreme values. Besides dissolution this can cause changes in morphology, both of which are known to affect the ordering of water molecules and ice nucleation ability. In this manuscript, we intend to demonstrate such effects on the structure of water that arise from aging of the surface and the variation of the solution composition due to freezing~~/~~ melting. We investigate the possible variation of the water- and ice- aerosol surface interactions with only one parameter in its environment which is the pH of the cloud droplet. We use fused silica surface as a model of mineral oxide aerosols.

Silicon is the most common element on earth after oxygen. In principle it may be present in the form of crystalline or amorphous SiO_2 or Si containing minerals. Both crystalline and amorphous forms of SiO_2 have been widely studied (Iler, 1979; Bergna and Roberts, 2005), also with interfacial behavior including silica~~/~~-water interface under static conditions using non-linear spectroscopy techniques (Ong et al., 1992; Ostroverkhov et al., 2004, 2005; Jena and Hore, 2009; Jena et al., 2011; Azam et al., 2012, 2013; Ohno et al., 2016; Dalstein et al., 2017; Darlington et al., 2017; DeWalt-Kerian et al., 2017; Schaefer et al., 2017; Boamah et al., 2018; Schaefer et al., 2018), potentiometric titration (Karlsson et al., 2001; Dove and Craven, 2005), Atomic Force Microscopy (Morag et al., 2013), or X-ray Photoelectron Spectroscopy (Brown et al., 2016). However, studies under non-equilibrium conditions are rare (Gibbs-Davis et al., 2008; Lis et al., 2014; Schaefer et al., 2018). Here, we are interested in fused silica, ~~which is~~ an amorphous form of SiO_2, under non-equilibrium conditions. From the point of view of surface chemistry, silica ~~has often been considered~~ is unusual ~~on the one hand side~~ because its surface charge characteristics ~~are different~~differ from ~~those of~~ many other mineral oxides ~~in the sense that~~. This is because classical silica charging curves involve a plateau at zero charge below about pH 5.5. ~~On the other hand silica~~ Silica also exhibits unusual aggregation behavior ~~and would remain~~, remains stable under conditions~~, where~~ that cause other mineral oxides ~~would~~to aggregate. A hairy like structure at the surface of colloidal silica has been advocated to explain this (steric stabilization). In the context of surface charging, silica has been often associated with a gel-like layer at its surface. The latter two aspects have been recently addressed in some detail ~~(Schrader et al., 2018). It was concluded from~~using surface force measurements ~~that neither indications for the~~(Schrader et al., 2018), but the proposed hairy ~~layer that has often been advocated as the explanation for the unusual stability nor evidence for the formation of a~~ and gel ~~layer could be~~ layers were not observed. Instead, the unusual behavior was explained by the heterogeneity of the surface ~~which in turn arises from the presence of~~caused by silanol (hydrophilic) and siloxane (hydrophobic) surface groups. To what extent these issues ~~are varying~~vary with chemical conditions (i.e. ~~exposure of a given surface for~~ long ~~times to a given solution, which might be more or less harsh, or~~term exposure of a given surface to ~~changing conditions over a long time) has not been frequently~~solutions) is poorly studied, ~~in particular when changing~~ particularly for temperatures between -40 and ~~25~~20 °C ~~are concerned~~. In this context ~~and taking up on the discussion above, the freezing and melting~~freeze-melt processes

involving a dilute solution at room temperature will result in ~~a solution during freezing and melting in contact with the surface~~solutions with a very high concentration of salt or acid/base in contact with the surface (see SI and Fig. S1).

~~The rates of quartz~~Quartz dissolution rates at 70 °C ~~at~~and pH 0 are as fast as at pH 8 to 10 (depending on the salt level) according to a comprehensive model by (Hiemstra and van Riemsdijk, 1990). The trend to increasing rates at very low pH (the rate minimum is at pH 3) is partially visible in some of the experimental data, and extrapolation suggests very fast dissolution at pH -1. The rates are also affected by the temperature, so that we here only use the available data and analogies to illustrate that dissolution is fast at very low pH values. This causes changes to the surface and should find repercussions in the surface properties. Surfaces of particles in the atmosphere undergo this kind of freeze~~/~~-melt cycles as well and therefore aged surfaces are probably much more relevant to ~~IN~~ice nucleation than the freshly prepared samples of the same particles that are typically used in laboratory work.

In this work, second-harmonic generation (SHG) was ~~utilized~~used to probe~~, on the~~ molecular-level~~, the change~~ changes in the ~~interfacial water~~ degree of ordering of interfacial water next to silica ~~surface~~surfaces being aged ~~via~~over multiple freeze-melt cycles~~ of freezing and melting.~~. We found that the surface water structure changes with both temperature ~~dependent restructuring of water molecules is changing with the~~and freeze-melt aging of the surface.~~ Freezing/melting cycles enhance the phenomenon.~~ The degrees of liquid water molecules ordering next to the surface at room temperature and shortly before freezing decrease and then increase again with sample aging. However, the water ordering–cooling dependence improves continuously with aging. This is accompanied with a continuous improvement in the ~~IN~~ice nucleation ability of the surface. We interpret the observed changes in the surface properties in terms of dissolution and re-adsorption of the dissolution products at the sample surface.

2 Experimental

MilliQ water (18.2 MΩ·cm) of total organic content below 4 ppb was used in all experiments. The pH solutions were freshly prepared before the experiments. The high and low pH solutions were prepared from NaOH and HCl (Sigma Aldrich), respectively. The bulk pH was measured at room temperature using a pH meter (Orion 720A+, Thermo electronic corporation) and a pH electrode (ORION 8102 BN, ThermoFisher Scientific). The pH measurement set-up was calibrated using buffers with known pH values. The pH value is temperature dependent since the dissociation constant of water changes with temperature (Bandura and Lvov, 2006; Zumdahl, 1993). The measuring cell was sealed from the lab environment to avoid dissolved gases in the liquid solutions. The concentration of dissolved Si ions in the solution after experiment was measured using inductively coupled plasma mass spectrometry (ICP-MS, X-Series II, ThermoScientific).

~~Fresh~~ For consistency, the data reported in this work were all collected on the same silica prism ~~like UV fused silica~~ sample (from Thorlabs GmbH~~)~~, optically polished UV fused silica, surface quality is 40-20 Scratch-Dig and surface flatness at 633 nm is Lambda/10). The fresh sample was cleaned first by soaking ~~it~~ in chloroform, acetone, and then ethanol (~ two hours each without sonication or 30 min with sonication, both giving the same result). Finally, the sample was flushed with MilliQ water. After each experiment series, the sample was cleaned with the same procedure, but excluding the chloroform step. Before starting ~~an~~ experimental ~~series (successive freezing / melting~~freeze-melt cycles~~),~~, the sample was soaked in ~~pH12~~pH 12 (NaOH) for 5 hours to generate a fresh surface ~~and finally in~~, followed by MQ water for another few hours and ~~then~~finally the sample washed with MQ water to remove excess sodium.

The SHG experiments were conducted using a 1 KHz femtosecond laser system (Solstice, Spectra Physics, 800 nm, 3.5 mJ, ~80 fs) with a beam diameter of ~2 mm at the interface. More details on the optical setup and the measuring cell can be found elsewhere (Abdelmonem et al., 2015; Abdelmonem et al., 2017; Abdelmonem, 2017). The fundamental beam was incident on the interface, Fig. 1, and the SHG signal was measured in co-propagating total internal reflection (TIR) geometry. A half-wave plate followed by a cube polarizer was used to adjust the polarization of the incident beam. The

generated signal was filtered, using a 400 nm band pass filter, before being measured using a photomultiplier tube (PMT). The measured signal amplitude at ~~certain~~a given polarization depends on the amount and structure of the interfacial molecules (Zhuang et al., 1999; Rao et al., 2003; Jang et al., 2013). It originates from the ~~nonresonant~~non-resonant electric dipolar contribution (Goh et al., 1988; Luca et al., 1995; Fordyce et al., 2001) and ~~proportionate to the incident field and the second-order nonlinear susceptibility $\chi^{(2)}$ of the interface.~~proportionates to the incident field and the second-order nonlinear susceptibility $\chi^{(2)}$ of the interface. It has been proven, for the water-silica system, that SHG is more sensitive to the number density of aligned water molecules, particularly at low pH and ionic strength (Rehl et al., 2019). For a charged interface, a third-order nonlinear polarization is induced by the static electric field due to the third-order nonlinear susceptibility $\chi^{(3)}$ of the solution (Ong et al., 1992; Zhao et al., 1993).

A silica prism was used as a sample where the hypotenuse was exposed to the solution. The incident angle of the fundamental beam was adjusted to 1° above the critical angle of TIR for silica-water interface to guarantee a TIR condition in the studied temperature range. In this work, the term Fresnel factors refers to nonlinear Fresnel factors affecting the SHG signal due to the optical constants of the media at the interface (Zhuang et al., 1999). The advantage of working close to the critical angle is that both PM (P-polarized SHG / 45°-polarized incident) and SM (S-polarized SHG / 45°-polarized incident) polarization combinations depend on only one non-vanishing nonlinear susceptibility tensor element (χ_{zzz}) and (χ_{yyz}), respectively (Shen, 1989; Zhuang et al., 1999). PM, however, gives a stronger signal and higher signal to noise ratio, and for this reason we only considered PM polarization. Nevertheless, we performed some runs with MP and MS ~~polarizations~~polarization combinations to assure that both give the same information (Fig. S2). The laser power coupled to the sample was 50 mW. The SHG signal is mainly produced by polarizable entities at the interface where the inversion symmetry is broken. Under TIR geometry, the contribution of polarizable molecules next to the solid surface is limited by the penetration depth inside the contact medium (gas, liquid or ice). The calculated penetration depths for air, liquid water, and ice in the above described geometry are about 143 nm, 720 nm, and 414 nm respectively. The time resolution of the SHG measurements is 2.5 sec. The standard deviation of the measurements is less than 10%.

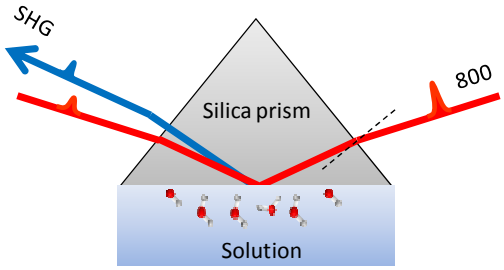

Figure 1: Sample and beams geometry (see text for details).

A cold stage (Linkam model HFS-X350) was used~~,~~ in a homemade temperature-controlled environmental chamber~~,~~ to apply a preset temperature profile (TP), and ~~the~~ SHG signal and substrate temperature were measured accordingly. In this work, we are not seeking ~~for~~ the exact onset freezing temperature, but rather the qualitative change of the freezing efficiency and the structural behavior of interfacial water molecules before, during, and after freezing. The silica prism was attached to the cold-stage and the surface of interest was exposed to the sample solution filled in a Teflon cell during the experiments. More details and ~~drawing~~drawings of the environmental chamber can be found elsewhere (Abdelmonem, 2017).

To allow qualitative comparisons, all results presented here were obtained using a standard TP, unless otherwise noted. For a standard run, the cell was filled with ~~1mL~~1 mL volume of the solution of interest. In each run, the silica sample was (1) kept in contact with the sample solution at 20 °C for 10 min, (2) cooled down to -40 °C at a rate of 5 °C/min, (3) held at -40 °C for 5 min, (4) heated up to 0 °C at a cooling rate of 20 °C/min, (5) held at 0 °C for 15 min to allow melting and departing of

the ice from the surface region, and (6) finally heated up to 20 °C at a rate of 20 °C/ min. This cooling profile was repeated ~~successively~~ to observe the changes in the freezing efficiency and water structure as a function of cooling cycle. The last two cycles were delayed for some hours to assess possible aging of the sample in contact with solution in the absence of freezing~~/ -~~melting effects. The ~~time~~duration of a complete standard TP is 45 min. In the following, the signal before freezing is labeled “liquid signal”, the peak at the freezing event is termed “transient freezing peak”, the signal after the freezing and transient freezing peak is labeled “ice signal”, the peak at the melting event is defined as “transient melting peak”, and the signal directly after the transient melting peak is termed ~~the~~ “confined liquid signal”.

3 Results and discussion

Figure 2 shows the SHG signal observed for pH = 3 solution in contact with silica surface as a function of time during 25 TP cycles. We chose pH = 3 because it is close to the point of zero charge ~~-~~of the used sample~~ and by that we eliminate~~, which eliminates the contribution from $\chi^{(3)}$. Also, at this pH the dissolution rate is ~~minimum as mentioned in the introduction~~minimized. Starting from 20 °C and cooling down, the liquid signal in cycle 1 gradually decreases with temperature until the freezing point. At the freezing point, we observe a transient signal upon freezing (a fast increase and subsequent decrease in the signal~~) upon freezing.~~). After freezing and at constant temperature, the ice signal ~~remains more or less~~is flat. After melting, we observe a high signal (confined liquid signal)~~ which lasts~~ for ~ 4 minutes. This period depends on the water volume and the holding time of ice at -40 °C. Finally, after heating back to 20 °C, we observe a liquid signal which is lower than the initial 20 °C liquid signal. When repeating the TP 25 times, we observe clear changes in the SHG-temperature dependence. The gradual decrease in the liquid signal with cooling before the freezing event gradually transforms to an increase. The liquid signal versus cooling decreases for the early TP cycles, remains constant during the intermediate TP cycles, and then increases for the later TP cycles, as indicated by the green arrows in Fig. 3. A transient melting peak becomes visible from TP cycle 5. Finally, after melting started and after the associated transient melting peak, we observe a signal from liquid confined between the surface and the remaining ice (confined liquid signal) the height of which decreases with the repeating TP cycles.

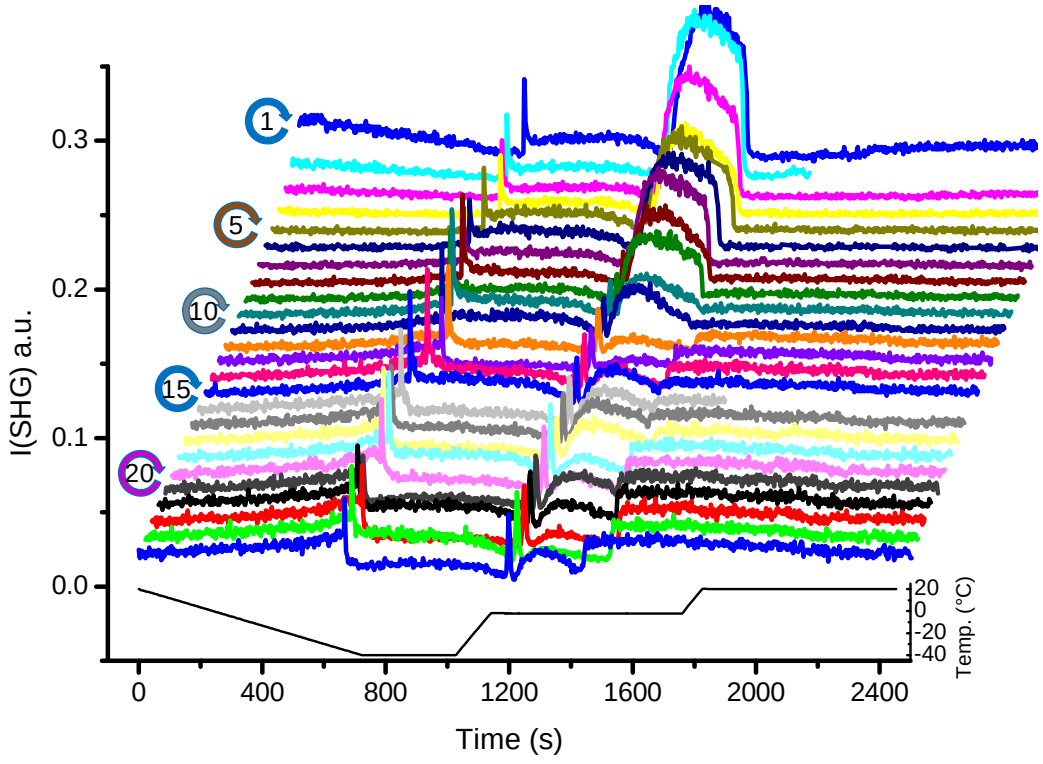

Figure 2: SHG signal at pH = 3 solution-silica interface as a function of time for 25 successive TP cycles. Due to technical problem, some data could be lost during the experiment (e.g. the not completed scans of cycle 2 and 16 in the presented set).

3.1 Liquid signal

~~In Figs. 2 and 3, the~~The SHG signal from time zero to the transient freezing peaks ~~show~~shows the liquid signal as a function of time ~~/~~vs. temperature during cooling from 20 °C to the freezing event~~.~~ (Figs. 2 and 3). This part of the TP indicates a restructuring of interfacial water as a function of temperature before freezing. In cycle 1, the liquid signal is relatively high at 20 °C (comparatively strongly ordered water molecules) and decreases with cooling indicating decreasing order in the water structure with decreasing temperature. This signal-temperature dependency weakens ~~with~~after repeating the TP. In cycle 5, the liquid signal remains almost constant during cooling. In cycle 10, the liquid signal starts to slightly increase with cooling, particularly before the freezing event. Finally, cycle 25 shows a significant increase in the water signal with cooling indicating that the surface induces a higher degree of water molecules ordering upon cooling.

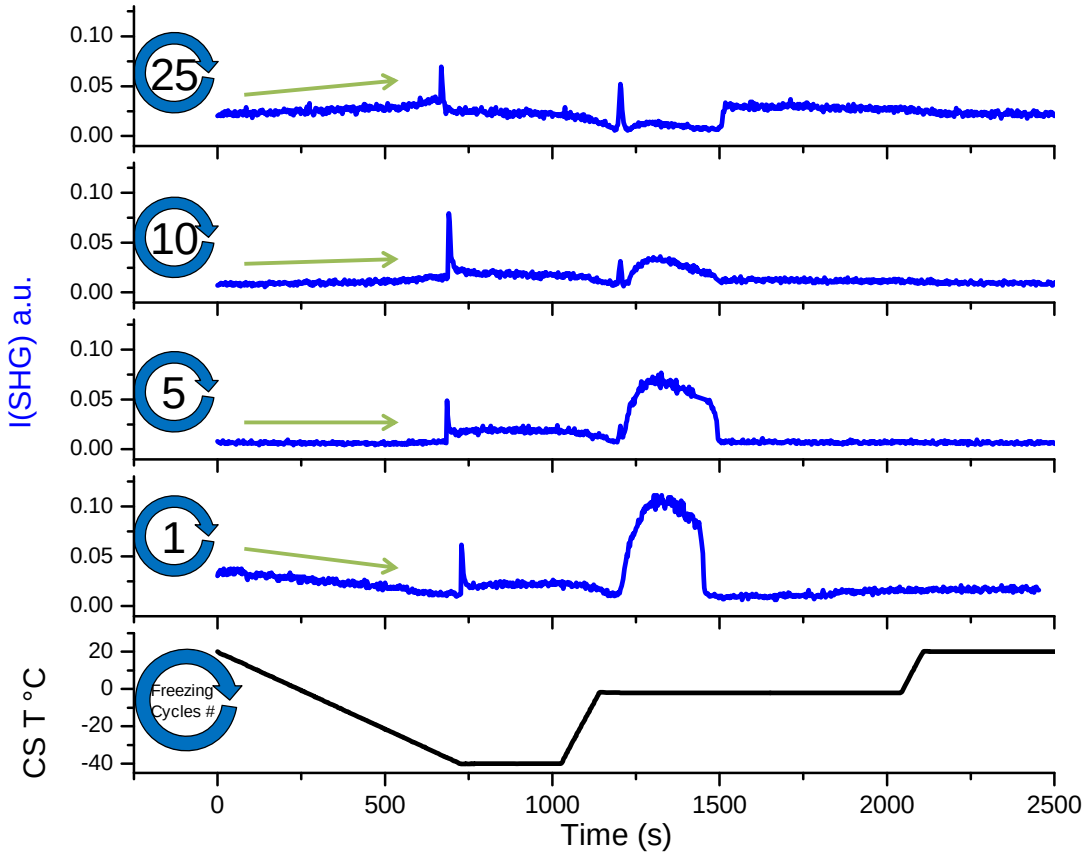

a) b)

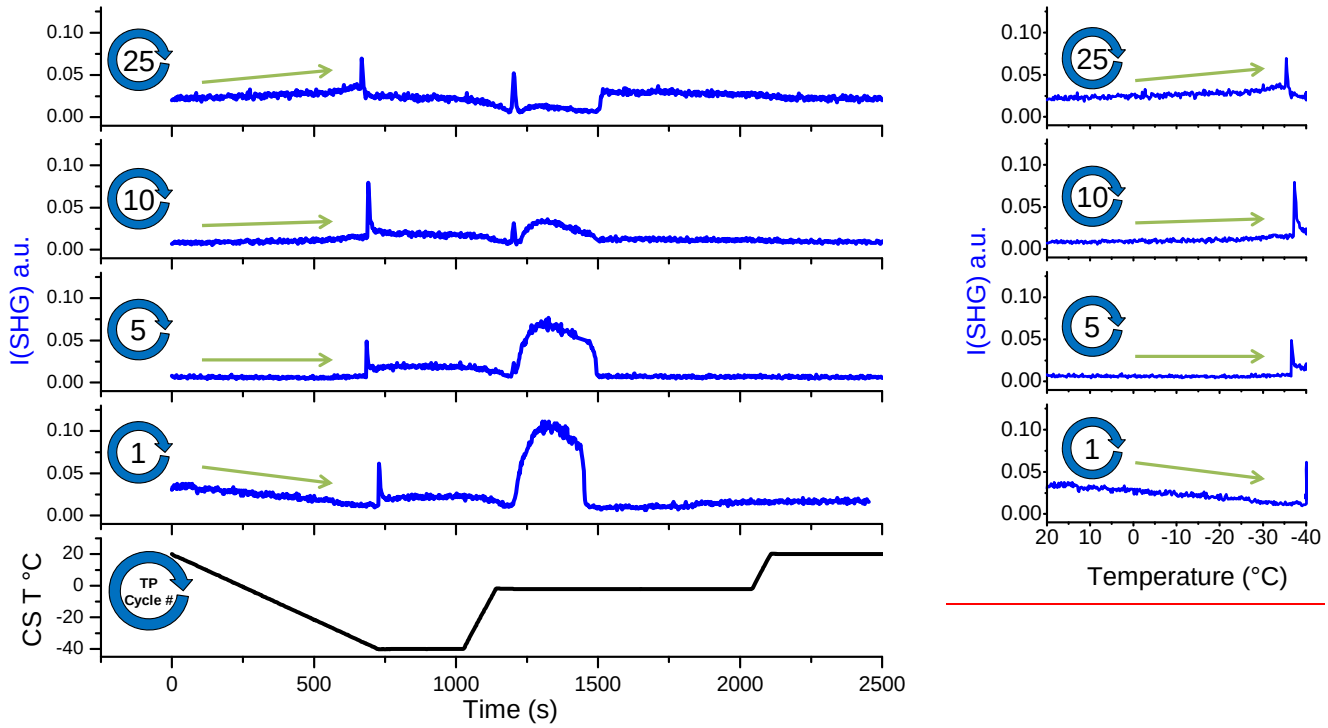

Figure 3: A selection from the set of plots shown in Fig. 2. (a) Temperature and SHG signal as a function of time. (b) SHG liquid signal as a function of temperature during cooling. This set of subplots shows clear change in the I(SHG) – temperature dependence during the TP iteration. CS T= Cold-stage temperature.

To gain more insight into the change in the water restructuring with temperature upon repeated TP cycles, we plot the SHG intensity as a function of cooling cycle at different temperatures. ~~Figure~~Figures 4a, b and c show the liquid signal as a function of TP cycle number at the beginning of each cycle (at 20 °C), shortly before the freezing event (at -31 °C), and immediately before the freezing event, respectively. The temperature of the latter slightly differs for each cycle. Additional plots at other temperatures can be found in SI3. Figure 4a shows a relatively high liquid signal at 20 °C in the first cycle. The 20 °C signal decreases and then increases again showing a minimum, located at approximately the 7th TP cycle, indicating a minimum degree of water molecules ordering at the interface in this cycle.

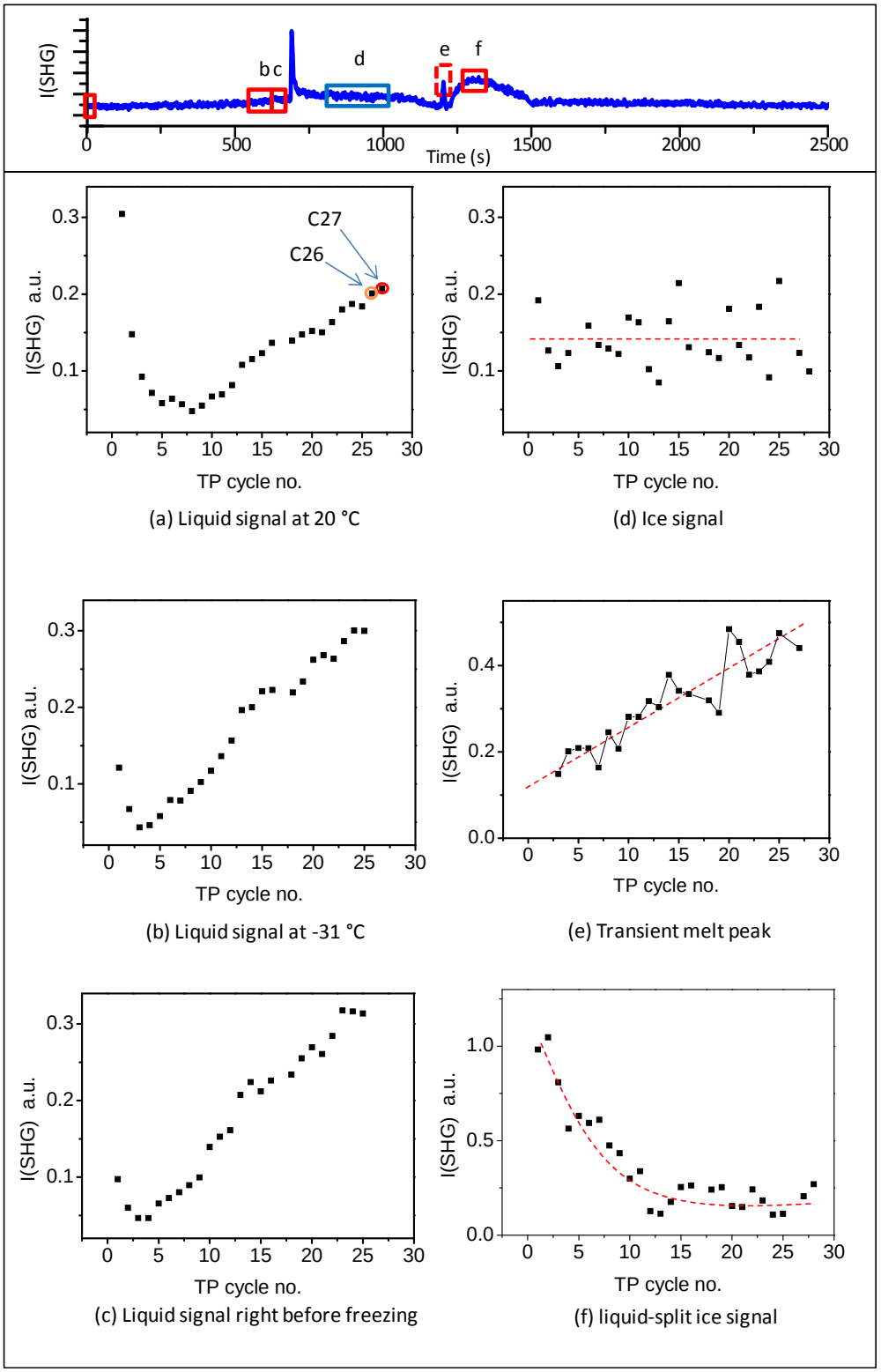

Figure 4: Upper panel: a sample plot of SHG vs. time during the standard TP. Lower panel: The averaged SHG signal as a function of TP cycle number at the different time slots marked with red and blue rectangles in the upper panel. The red rectangle corresponds to liquid phase while the blue rectangle corresponds to ice phase. The dashed red lines on the plots are guiding lines through the data points.

The cycles from 1 to 25 have been carried out with equal time intervals. However, to assure that the changes we observe here are mainly due to the freezing/-melting effect and not simply time dependent surface aging in contact with pH = 3 solution, we carried out two additional cycles after deliberately waiting for 5 hours while the sample was in contact with pH = 3 at room temperature. This time is equivalent to the time needed to perform about 6 TP cycles. The 20 °C liquid signals of these two additional cycles are marked as orange (C26) and red (C27) circles in Fig. 4a. C26 has the same standard TP of the preceding 25 cycles while the red C27 has a different TP for a reason to be discussed later. By comparing the plot of the SHG signal vs. cooling cycle number (Fig. 4a), and vs. time (Fig. S3S4), we find that the two data points of the two additional cycles (C26 and C27) fit well with the extrapolation of the changes in the SHG signals with TP cycle number. However, these two points are offset in terms of time when extrapolating the SHG signal with time. We conclude that the changes in the surface–solution system are accelerated by the freezing and melting processes. It is well established that silica surfaces dissolve in aquatic environments (Hiemstra and van Riemsdijk, 1990). As mentioned in the introduction, dissolution is accelerated by very low and high pH values. The amount of aqueous silica depends on the pH and the time of exposure. However, the observed changes in the 20 °C SHG signal as a function of TP cycle number, Fig. 4a, within the relatively short time intervals, about 45 min per cycle, can only be attributed to an accelerated dissolution upon freezing/-melting followed by re-adsorption of dissolution products, hence changing the surface properties which in turn influences the interfacial water structure.

The decrease and subsequent increase in the liquid signal at 20 °C with the progress of the TP cycles,- (Fig. 4a,) can be explained as follows: At the beginning, before the minimum point, adsorbed dissolution products interrupt the water structure which is expected to be slightly ordered due to the H-bonding or the weak surface charge at pH = 3. As mentioned above, pH = 3 is close to the point of zero charge of silica and therefore the signal is low compared to neutral or high pH, Fig. S4S5. Each freezing/-melting cycle increases the concentration of the dissolution products in the bulk solution sufficiently to change the ionic strength of the interfacial water and this in turns affects the interfacial water structure. At the minimum point, adsorbate concentration at the surface causes the highest disorder of the water molecules. Beyond the minimum point, the adsorbate concentration is sufficiently high to induce a certain degree of arrangement of water molecules. This results in an increase of the liquid signal at 20 °C beyond the minimum point. The alteration of the signal trend originates from an interplay between screening and interference effects (Schaefer et al., 2017). In the following, the interaction before the minimum point will be termed a “screening phase” and that after minimum an “interference phase”.

Shortly before the freezing event the liquid signal as a function of TP cycle number also shows a minimum as can be seen in the Fig. 4b and c, respectively. Figure 4b shows the SHG liquid signal at -31 °C while Fig. 4c shows the signal immediately before the freezing point, for all TP cycles. Figures 4b and c show similar behavior. In both cases the minimum point occurs between cycles 3 and 4, i.e. not at the same position as the minimum point of the 20 °C liquid signal (around cycle 7). This suggests that temperature affects the adsorption-desorption balance. The effect of re-adsorption, on water structure before the minimum point, at lower temperature precedes that at higher temperature- (Figs. 4a-c, S3a-e). This means that cooling favors the uptake of dissolved silica (i.e. adsorption) and hence increases the interfacial ion concentration. Considering the thermodynamic behavior of silica in such systems (see SI1, Fig. S1) the solubility of amorphous silica strongly decreases with decreasing temperature. Adsorption of inorganic solutes to mineral oxide surfaces is typically strongly related to the solubility behavior (Lützenkirchen and Behra, 1995) so that the thermodynamic calculations in SI support the idea of enhanced re-adsorption of dissolved silica enhances the re-adsorption to the fused silica surface under cooling. This justifies the hypotheses that the change in the liquid signal with an increasing number of TP cycles is due to the uptake of dissolved silica ions. The decrease in liquid signal with temperature decrease within the screening phase is consistent with the conclusion that in this phase re-adsorption causes disorder of water molecules and that cooling accelerates the completion of this phase.

Beyond the minimum, the older the ~~sample~~surface, i.e. the more frequently exposed to freezing-melting cycles, the higher the degree of ordering induced by the surface on the interfacial water particularly at supercooled condition. In addition, the liquid signal-temperature dependence per TP cycle converts from inversely to directly proportional with cooling (green arrows in Fig. 3). It has been shown in different studies on water-mineral oxide interface that a higher degree of ordering of liquid water molecules next to the surface is an indication of higher heterogeneous freezing efficiency (Abdelmonem, 2017; Abdelmonem et al., 2017; Abdelmonem et al., 2015; Anim-Danso et al., 2013; Anim-Danso et al., 2016; Yang et al., 2011). In the present work, it was our intention to impose a constant cooling rate to qualitatively follow the freezing efficiency and interfacial water structural changes under identical conditions. Figure 5 shows the freezing temperatures obtained under the standard TP and experimental conditions described above. The overall trend shows that the older the ~~sample~~surface the higher the temperature of freezing, i.e. the earlier the freezing event, under the same conditions. This means that indeed the aged sample exhibits better ~~IN~~ice nucleation efficiency which is induced by the pre-structuring of water molecules by the modified surface.

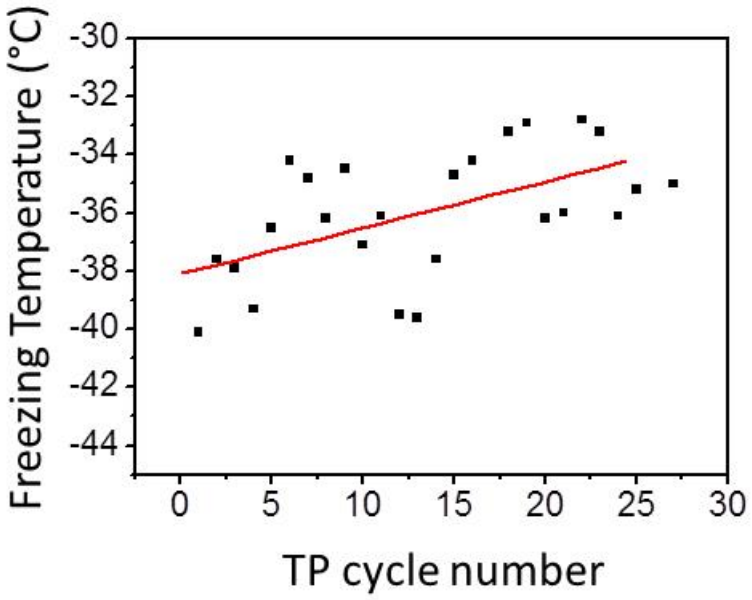

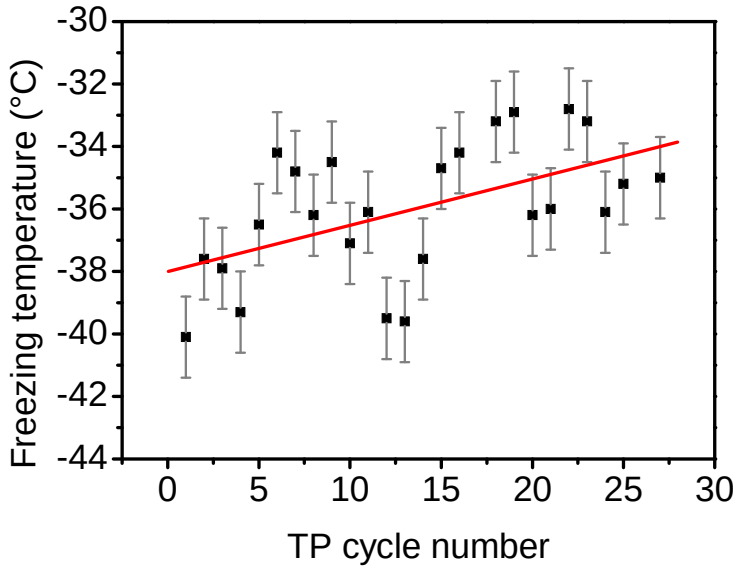

Figure 5: Freezing temperature of pH = 3 solution as a function of the TP cycle number under the experimental conditions mentioned in the text. Black squares represent experimental data. Red line is a linear fit to follow the trend of the data points. The error bars have been evaluated from the standard deviation of different experiments.

For quantification we need to find the range of bulk concentrations at which we may observe alteration in the signal behavior. As a control experiment, we prepared dissolved silica solutions with different concentrations of silicic acid at pH = 3 and measured the SHG signal at the interface for each solution at room temperature. Figure 6 shows the SHG intensity as a function of ~~ion~~silica concentration. Indeed, we observe oscillations in the signal as the silica concentration increase. Without invoking any model, this directly supports the conclusion that the change in the SHG signal in our freezing~~/~~-melting experiments was due to the change in the dissolution products concentration with the progress of the TP cycles. The minimum we see in Fig. 4a should correspond to one of the minima in the silica ions concentration experiment, Fig. 6. By analyzing the pH = 3 solution in contact with the silica surface after the complete set of TP cycles, we found that the aqueous concentration of Si was 41.0 ± 1.5 µM. This means that by repeating the freezing~~/~~-melting TP cycle the dissolution products generated a substantial interfacial ionic strength equivalent to that at the low concentration range of Fig. 6 (shadowed area). The dissolution of silica changed the z-dependent electrostatic potential of the bare silica~~/~~-water interface in a very similar manner as the addition of approximately 41µM silicic acid at pH = 3 at room temperature, implying an interfacial concentration of dissolution-released entities of the same order. This control experiment corroborates the scenario of multi adsorption phases of dissolution products at the surface and the concomitant effect it has on the water structure.

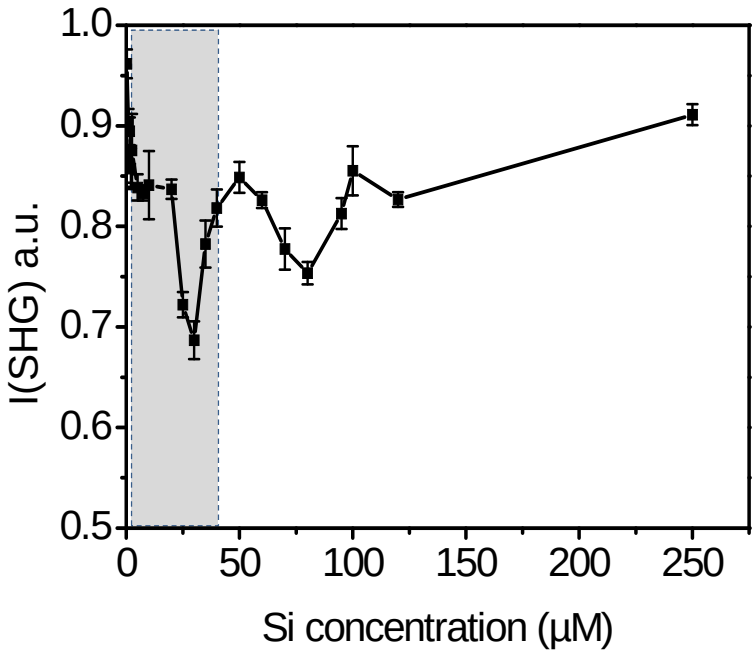

Figure 6: SHG intensity as a function of silica ions concentration at pH = 3 at 20 °C. The error bars represent the standard deviation from the corresponding average value.

3.2 Transient freezing and melting peaks

Although this study was not aimed at discussing the transient freezing peak, the obtained data enforce us to reconsider this recently observed ambiguous phenomenon. The transient peak upon freezing was reported at ~~pH9~~pH 9.8 for the aqueous solution-mica interface using SFG spectroscopy (Anim-Danso et al., 2016), for a neutral water-silica interface using SFG spectroscopy (Lovering et al., 2017), for a neutral water-mica and -sapphire interface using SHG spectroscopy (Abdelmonem, 2017), and for a ~~pH9~~pH 9 aqueous solution-sapphire interface using SFG spectroscopy (Abdelmonem et al., 2018). Anim-Danso et al. supposed that the transient signal is due to progressive events occurring near the surface during the phase transition without specifying a potential process. Lovering et al. suggested the presence of a transient stacking-

disordered ice at the interfaces during freezing. Abdelmonem et al. (2018) have reported that the observed transient signals arise from a smooth transition between water and ice and does not necessarily indicate transient species. It was demonstrated that the transient change in the signal intensity results from an interference between different SFG peak parameters changing at different rates. All SFG and SHG studies mentioned above showed a transient increase in the signal, although with different temporal characteristics (few tens of seconds to several minutes).

In the present study ~~we adjudicate on this debate and~~, we provide evidence that the transient freezing peak arises from ~~the~~a multi-interface problem, and the reported observations may indeed be explicable without the need to invoke any transient species. We also address the parameters affecting the transient time. In our experiments we observed the transient signal at freezing and melting as well. To interpret the transient signal we corrected our data for the Fresnel factors. Figure 7 shows the corrected and non-corrected SHG signal around the transient freezing and transient melting peaks of TP cycle number 25. The liquid data before the transient freezing peak and after the transient melting peak are corrected to the water Fresnel factors (red lines) and the ice data between the transient freezing peak and the transient melting peak are corrected to the ice Fresnel factors (blue lines). All corrected data sets have then been normalized to the measured ice signal for the sake of clearness. For this reason, the Fresnel corrected ice data (blue lines) coincide with the non-Fresnel corrected signal (black solid circles). The lower panels of Fig. 7 show a schematic representation of the development of the ice forming and melting at the interface around the freezing and melting events, respectively, involving six steps: 1. Before the freezing event, the SHG signal arises from the liquid-solid interface and is affected by the Fresnel factors of bulk liquid and bulk solid (silica). 2. Once ~~the~~ freezing occurs, a thin film of ice is formed at the surface. This film is sufficiently thin for the ice-solid interface SHG signal to be still affected by the Fresnel factors of bulk liquid and bulk solid. 3. After the freezing event, the ice film grows and the SHG signal is generated from the ice-solid interface and affected by the Fresnel factors of bulk ice and bulk solid. 4. Before the melting event (similar to 3). 5. Once the melting occurs, a thin film of liquid is formed at the surface. This film is sufficiently thin so that the SHG signal at liquid-solid interface is still affected by the Fresnel factors of bulk ice and bulk solid. 6. Later after the melting event, the ice melts further and the SHG signal is generated from the liquid-solid interface and affected by the Fresnel factors of bulk liquid and bulk solid.

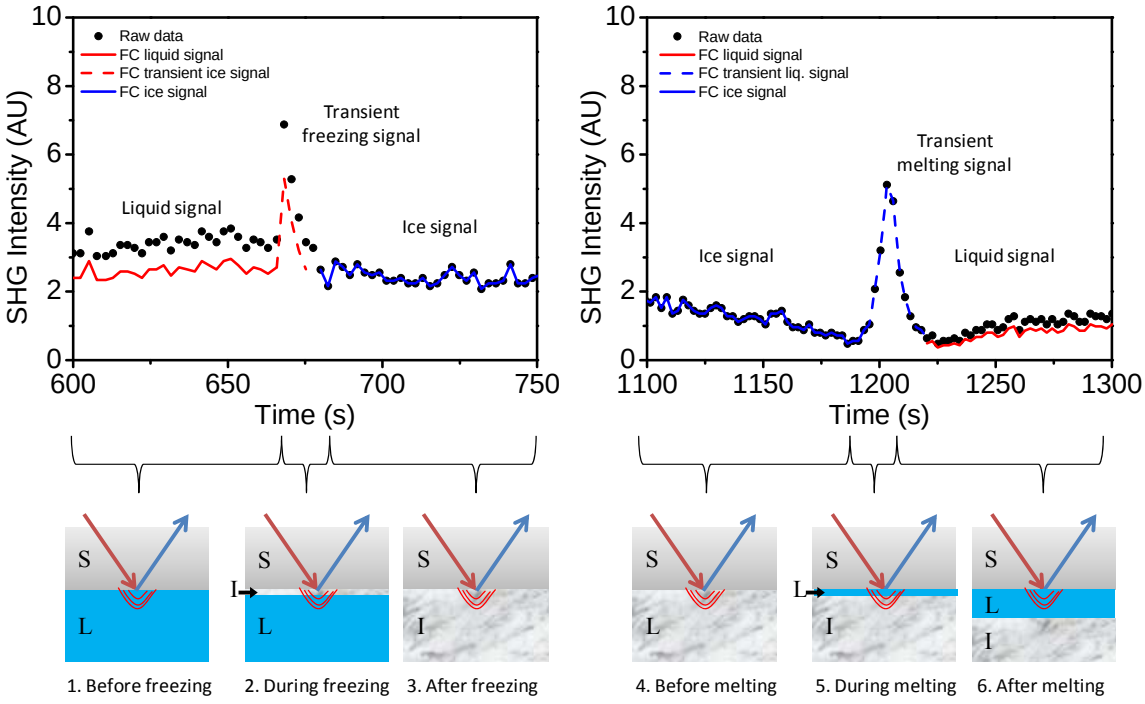

Figure 7: Upper panel: A comparison between SHG signal, corrected (continuous and dashed lines) and non-corrected (black solid circles) to the Fresnel factors, around the transient freezing peak (left panel) and around the transient melting peak (right panel) for TP cycle

number 25. Red lines correspond to liquid phase, blue lines correspond to ice phase, and dashed lines correspond to transient signal. Lower panel: A schematic representation of the development of the ice forming and melting at the interface around freezing and melting events, respectively.

The transient signals persist until the respective ice or liquid film thickness exceeds the evanescent field (represented by the red bows at the interfaces in the lower panel of Fig. 7). Considering the transient freezing, if we assume that the bulk liquid optical constants are the origin of the transient ice signal, ~~then correcting~~and correct for the transient ice signal to liquid-solid Fresnel factors, the maximum signal should ~~lead to a maximum not higher~~be less than the ice signal~~, but~~. But this is not the case. Correcting the transient ice signal to the liquid-solid Fresnel factors gives the dashed red line in Fig. 7, which has a maximum significantly higher than the ice signal. Similar justification applies to the transient melting if we correct the transient liquid signal to the ice-solid Fresnel factors (dashed blue line in Fig. 7). Thus, the Fresnel Factor corrections cannot exclusively explain the transient freezing behavior.

We conclude here that the effect of the Fresnel Factors, or in other words the optical constants of the bulk isotropic media around the interface, is not sufficient to generate the observed transient peak. However, another multi-interface problem is accompanying the formation and growth of ice and liquid films after the freezing and melting events~~, respectively.~~. In the case of freezing, once ~~the IN~~ice nucleation starts and until the thickness of the ice film exceeds the depth of the evanescent field, two interfaces are involved and can contribute directly to the signal: the ice-solid interface and the liquid-ice interface (see drawing 2 in the lower panel of Fig. 7). The SHG signal of the first interface (ice-solid) should be comparable to that of the ice signal (blue line, upper left panel, Fig. 7). ~~The~~However, the SHG signal of the second interface (liquid-ice~~), however,~~) is an additional contribution to the detected signal, which emerges for a very short time (i.e. the time of vertical growth of the ice film within the evanescent field). In the case of melting, before the thickness of the liquid film exceeds the depth of the evanescent field, (drawing 5, lower panel, Fig. 7) an additional temporary signal from the ice-liquid interface is contributing to the liquid-solid interface. Again, the ice-liquid signal should be sufficiently higher than that of the liquid-solid interface at pH ~~=~~3, and will last for a short time until the liquid layer thickness exceeds the evanescent field. The signal generated at the secondary interface has not been considered in the ~~above discussed~~ SFG and SHG studies discussed above.

We also believe that this transient signal occurs in all similar systems, while its detection depends on data acquisition speed and the geometry of the measuring cell. The data represented here were collected at time resolution of 2.5 sec. If the time resolution would be ~~greater than~~above 9 sec, which is the average duration of the transient freezing peaks under our standard TP, a transient freezing signal would not be observable for this system. The transient time depends on the experimental conditions of the system, e.g. the cooling rate, the sample volume and the thermal conductivities of the two isotropic media. At the melting event, a thin water film is formed between solid and ice which starts to grow vertically at the expense of the ice melting (drawing 5, lower panel, Fig. 7). A quasi liquid layer has been reported on the ice surface in both atmospheric ice and multiphase chemistry as well as in commercial contexts. The growth of such a film is, however, slower than the growth of the ice film after freezing, because the energy transfer between solid surface and ice is slower than that between the solid surface and water. The vertical growth of the thin water film formed upon melting is then expected to last for a relatively longer time than that of the ice sheet after the freezing event. Indeed, the average transient melting time was about 16 seconds in our standard TP (cycles from 1 to 25). We tested the heat transfer effect in one very slow cooling profile (TP of C27) which is shown in Fig. ~~S5~~S6. The very slow cooling ~~evolved~~involved enough time for the bulk liquid to cool down, enhancing by this the vertical ice growth rate compared to the standard TP used for runs 1 to 25. Once the freezing occurred in C27, the propagation of the ice in the z direction was so fast that the 2.5 sec resolution of the detection system was not able to detect the transient freezing signal. Although no transient freezing temperature was observed in C27, the transient melting peak was detected for this TP cycle and was even longer (~ 48 sec) than for the first 25 cycles of the standard TP. This is because the longer cooling time developed a larger ice bulk in the measuring cell, i.e., a bigger heat absorber than the bulk ice in the standard TP cycles. This generates more resistance to the growth of the thin water film.

In summary, we conclude that the transient SHG/SFG signals observed in the above mentioned studies were a result of the multi-interface problem. However, using such a signal under controlled conditions can allow for measuring crystal growth which is so far a challenging task due to the incomplete understanding of the physical mechanisms underlying ice crystallization. It is worth to notice here that the height of the transient melting peak is proportional to the sample aging caused by successive TP cycles and, in our system, starts after cycle 3, Fig. 4e. This corroborates the role of the interference phase after the minimum point as discussed in the liquid signal section. We have not attempted to plot the ~~transit~~transient freezing peak height in Fig. 4. Due to the limited detection time resolution and the fast change in the transient freezing signal, the peak region involved only one data point from which the actual peak height cannot be determined. With this we presented a reasonable interpretation of the transient signal which ~~was~~has been under debate in the recent years.

3.3 ~~Ice~~Confined liquid and ice signal

The ice signal~~, Fig. 4d,~~ did not show any clear trend with repeating the TP~~. However~~ (Fig. 4d), but we noticed a strong ~~fluctuations~~fluctuation in the level of the averaged ice signal after the freezing. This ice signal fluctuation merits further investigations particularly using SFG which gives details on the individual contributions of different interfacial species from their resonant vibrations.

~~3.4 Confined liquid~~

The confined liquid signal, labelled (f) in the upper panel of Fig. 4, is generated at the interface between the silica surface and bulk liquid confined between the silica surface and ice after melting a relatively thick interfacial layer (drawing 6 lower panel, Fig. 7). This confined bulk liquid is sufficiently thick for the evanescent field not to reach the bulk ice. It is hence a signal only generated at the liquid-solid interface. This signal is strongly influenced by the geometry of our experiment and can change from one cell design to another (see Fig. ~~S6~~S7). In our cell design, the ice piece which separates from the sample surface after melting stays close to the surface and requires some time to be detached from the interfacial region and move towards the unfrozen water ~~not been frozen~~ during the experiment (see Fig. ~~S6~~S7). Although this piece of ice does not contribute directly to the signal, it indirectly influences the SHG signal as a result of two simultaneous effects: 1. Depending on the distance between this ice piece and the surface, the orientation of the interfacial water may be influenced by the ice surface. 2. The melting of this ice piece slowly dilutes the solution back to pH ~~=~~ 3. The combination of these two simultaneous processes ~~result~~results in the hump we see in the SHG curves~~, Fig. 2 and 3,~~ in the region after the transient melting peak~~.~~ (Fig. 2 and 3). A supplementary video~~,~~ shows the development of this hump with the melting and motion of ~~this~~the ice piece ~~from after the~~during melting ~~event to complete melting,~~ is available (Abdelmonem et al., 2019). The height of the confined liquid signal decreases ~~with~~upon repeating the TP~~,~~ (Fig. 4f~~.~~). This ~~is an~~provides additional evidence that the surface-solution system is significantly changing with the iteration of the TP. Regardless of the vague behavior of the confined liquid signal, optimizing this setup may ultimately allow us to extend our studies to investigate interfacial water melted between ice and solid surface or the so called quasi-liquid layer (Nagata et al., 2019; Li and Somorjai, 2007; Rosenberg, 2005; Döppenschmidt et al., 1998), which ~~receives strong interest from different~~also has industrial applications (e.g. ski sports, frozen food packaging~~,...).~~).

4 Conclusions

~~The~~We studied the effect of surface aging under acidic conditions on the rearrangement of interfacial water molecules next to an amorphous silica surface ~~has been studied~~ at the molecular level using SHG spectroscopy under temperature-controlled conditions. The aging ~~has been~~was accelerated by successive ~~freezing / melting~~freeze-melt cycles of a pH ~~=~~ 3 solution ~~next to~~in contact with the surface. Similar aging is highly probable for mineral oxide aerosols in the atmosphere. The aging altered the temperature dependence of the water structure ~~next to the surface~~ and ~~correspondingly the~~ ice nucleation ability

of the surface. ~~The~~ We interpreted the alteration in the water-silica interaction ~~could be understood~~ in terms of the disruption of the equilibrium at the surface due to dissolution and re-adsorption of dissolution products. The re-adsorption of dissolved silica generates a network on the surface. The SHG intensity versus freeze-melt cycle number at constant temperature indicated alteration in the generated network. A control experiment showed an oscillation in the degree of order of water molecules with Si ion concentration. The first minimum in this oscillation quantified the dissolution-released entities in the aging experiments. Beside the main findings, we ~~gave~~provided a reasoning explanation of the transient freezing and melting signals, which were recently observed by SFG and SHG studies~~,~~ on similar systems, and were questioned in terms of reality and origin. ~~The~~Our results provide new insights in ~~our~~the understanding of the consequences of surface aging in aqueous solutions ~~and~~ under atmospheric conditions. This study is expected to benefit future atmospheric research, particularly cloud formation and aerosol aging in the atmosphere, with potential implications for ~~the~~ pharmaceutical and food industries.

ASSOCIATED CONTENT

Supporting Information. The supporting information comprises thermodynamic considerations, and associated data and plots. This material is available free of charge via the Internet at.

AUTHOR INFORMATION

Corresponding Authors

E-mail: ahmed.abdelmonem@kit.edu,

Conflicts of interest

There are no conflicts to declare.

ACKNOWLEDGMENTS

AA is grateful to the German Research Foundation (DFG, AB 604/1-1,2). SR thanks the DAAD (2017/18, 57299294). The authors are grateful to Mischa Bonn for useful discussions and acknowledging Horst Geckeis, Thomas Leisner, Frank Heberling, Dieter Schield and Teba Gil-Diaz for their support.

References

Abdelmonem, A., Lützenkirchen, J., and Leisner, T.: Probing Ice-Nucleation Processes on the Molecular Level using Second Harmonic Generation Spectroscopy, Atmos. Meas. Tech., 8, 3519-3526, doi: 10.5194/amt-8-3519-2015, 2015.

Abdelmonem, A.: Direct Molecular-Level Characterization of Different Heterogeneous Freezing Modes on Mica – Part 1, Atmos. Chem. Phys., 17, 10733-10741, doi: 10.5194/acp-17-10733-2017, 2017.

Abdelmonem, A., Backus, E. H. G., Hoffmann, N., Sánchez, M. A., Cyran, J. D., Kiselev, A., and Bonn, M.: Surface-Charge-Induced Orientation of Interfacial Water Suppresses Heterogeneous Ice Nucleation on α-Alumina (0001), Atmos. Chem. Phys., 17, 7827-7837, doi: 10.5194/acp-17-7827-2017, 2017.

Abdelmonem, A., Backus, E. H. G., and Bonn, M.: Ice Nucleation at the Water–Sapphire Interface: Transient Sum-Frequency Response without Evidence for Transient Ice Phase, J. Phys. Chem. C, doi: 10.1021/acs.jpcc.8b07480, 2018.

Abdelmonem, A., Ratnayake, S., and Lützenkirchen, J.: Melting_Peak-Hump.avi, doi: 10.6084/m9.figshare.9878369.v1, 2019.

Anim-Danso, E., Zhang, Y., Alizadeh, A., and Dhinojwala, A.: Freezing of Water Next to Solid Surfaces Probed by Infrared-Visible Sum Frequency Generation Spectroscopy, J. Am. Chem. Soc., 135, 2734–2740, doi: 10.1021/ja311648q, 2013.

Anim-Danso, E., Zhang, Y., and Dhinojwala, A.: Surface Charge Affects the Structure of Interfacial Ice, J. Phys. Chem. C, 120, 3741-3748, doi: 10.1021/acs.jpcc.5b08371, 2016.

Azam, M. S., Weeraman, C. N., and Gibbs-Davis, J. M.: Specific Cation Effects on the Bimodal Acid–Base Behavior of the Silica/Water Interface, J. Phys. Chem. Lett., 3, 1269-1274, doi: 10.1021/jz300255x, 2012.

Azam, M. S., Weeraman, C. N., and Gibbs-Davis, J. M.: Halide-Induced Cooperative Acid–Base Behavior at a Negatively Charged Interface, J. Phys. Chem. C, 117, 8840-8850, doi: 10.1021/jp401164r, 2013.

Bandura, A. V. and Lvov, S. N.: The Ionization Constant of Water over Wide Ranges of Temperature and Density, J. Phys. Chem. Ref. Data, 35, 15-30, doi: 10.1063/1.1928231, 2006.

Bergna, H. E. and Roberts, W. O.: Colloidal Silica: Fundamentals and Applications, Surfactant Science, CRC Press, Boca Raton, 2005.

Boamah, M. D., Ohno, P. E., Geiger, F. M., and Eisenthal, K. B.: Relative permittivity in the electrical double layer from nonlinear optics, J. Chem. Phys., 148, 222808, doi: 10.1063/1.5011977, 2018.

Brown, M. A., Goel, A., and Abbas, Z.: Effect of Electrolyte Concentration on the Stern Layer Thickness at a Charged Interface, Angew. Chem. Int. Ed., 55, 3790-3794, doi: 10.1002/anie.201512025, 2016.

Coluzza, I., Creamean, J., Rossi, M. J., Wex, H., Alpert, P. A., Bianco, V., Boose, Y., Dellago, C., Felgitsch, L., Frohlich-Nowoisky, J., Herrmann, H., Jungblut, S., Kanji, Z. A., Menzl, G., Moffett, B., Moritz, C., Mutzel, A., Poschl, U., Schauperl, M., Scheel, J., Stopelli, E., Stratmann, F., Grothe, H., and Schmale, D. G.: Perspectives on the Future of Ice Nucleation Research: Research Needs and Unanswered Questions Identified from Two International Workshops, Atmosphere, 8, doi: 10.3390/atmos8080138, 2017.

Cox, J. R., Ferris, L. A., and Thalladi, V. R.: Selective Growth of a Stable Drug Polymorph by Suppressing the Nucleation of Corresponding Metastable Polymorphs, Angew. Chem. Int. Ed., 46, 4333-4336, doi: 10.1002/anie.200605257, 2007.

Cox, S. J., Raza, Z., Kathmann, S. M., Slater, B., and Michaelides, A.: The microscopic features of heterogeneous ice nucleation may affect the macroscopic morphology of atmospheric ice crystals, Faraday Discuss., 167, 389-403, doi: 10.1039/c3fd00059a, 2013.

Dalstein, L., Potapova, E., and Tyrode, E.: The elusive silica/water interface: isolated silanols under water as revealed by vibrational sum frequency spectroscopy, Phys. Chem. Chem. Phys., 19, 10343-10349, doi: 10.1039/c7cp01507k, 2017.

Darlington, A. M., Jarisz, T. A., DeWalt-Kerian, E. L., Roy, S., Kim, S., Azam, M. S., Hore, D. K., and Gibbs, J. M.: Separating the pH-Dependent Behavior of Water in the Stern and Diffuse Layers with Varying Salt Concentration, J. Phys. Chem. C, 121, 20229-20241, doi: 10.1021/acs.jpcc.7b03522, 2017.

DeWalt-Kerian, E. L., Kim, S., Azam, M. S., Zeng, H., Liu, Q., and Gibbs, J. M.: pH-Dependent Inversion of Hofmeister Trends in the Water Structure of the Electrical Double Layer, J. Phys. Chem. Lett., 8, 2855-2861, doi: 10.1021/acs.jpclett.7b01005, 2017.

Döppenschmidt, A., Kappl, M., and Butt, H.-J.: Surface Properties of Ice Studied by Atomic Force Microscopy, J. Phys. Chem. B, 102, 7813-7819, doi: 10.1021/jp981396s, 1998.

Dove, P. M. and Craven, C. M.: Surface charge density on silica in alkali and alkaline earth chloride electrolyte solutions, Geochim. Cosmochim. Acta, 69, 4963-4970, doi: https://doi.org/10.1016/j.gca.2005.05.006, 2005.

Fordyce, A. J., Bullock, W. J., Timson, A. J., Haslam, S., Spencer-Smith, R. D., Alexander, A., and Frey, J. G.: The temperature dependence of surface second-harmonic generation from the air-water interface, Mol. Phys., 99, 677-687, doi: 10.1080/00268970010030022, 2001.

Gibbs-Davis, J. M., Kruk, J. J., Konek, C. T., Scheidt, K. A., and Geiger, F. M.: Jammed Acid−Base Reactions at Interfaces, J. Am. Chem. Soc., 130, 15444-15447, doi: 10.1021/ja804302s, 2008.

Goh, M. C., Hicks, J. M., Kemnitz, K., Pinto, G. R., Heinz, T. F., Eisenthal, K. B., and Bhattacharyya, K.: Absolute orientation of water molecules at the neat water surface, J. Phys. Chem., 92, 5074-5075, doi: 10.1021/j100329a003, 1988.

Harrison, A. D., Whale, T. F., Carpenter, M. A., Holden, M. A., Neve, L., O'Sullivan, D., Vergara Temprado, J., and Murray, B. J.: Not all feldspars are equal: a survey of ice nucleating properties across the feldspar group of minerals, Atmos. Chem. Phys., 16, 10927-10940, doi: 10.5194/acp-16-10927-2016, 2016.

Hiemstra, T. and van Riemsdijk, W. H.: Multiple activated complex dissolution of metal (hydr) oxides: A thermodynamic approach applied to quartz, J. Colloid Interface Sci., 136, 132-150, doi: https://doi.org/10.1016/0021-9797(90)90084-2, 1990.

Holden, M. A., Whale, T. F., Tarn, M. D., O'Sullivan, D., Walshaw, R. D., Murray, B. J., Meldrum, F. C., and Christenson, H. K.: High-speed imaging of ice nucleation in water proves the existence of active sites, Sci. Adv., 5, eaav4316, doi: 10.1126/sciadv.aav4316, 2019.

Hoose, C. and Mohler, O.: Heterogeneous ice nucleation on atmospheric aerosols: a review of results from laboratory experiments, Atmos. Chem. Phys., 12, 9817-9854, doi: 10.5194/acp-12-9817-2012, 2012.

Iler, R. K.: The Chemistry of Silica: Solubility, Polymerization, Colloid and Surface Properties and Biochemistry of Silica, John Wiley & Sons Inc, New York, 1979.

Jang, J. H., Lydiatt, F., Lindsay, R., and Baldelli, S.: Quantitative Orientation Analysis by Sum Frequency Generation in the Presence of Near-Resonant Background Signal: Acetonitrile on Rutile TiO2 (110), J. Phys. Chem. A, 117, 6288-6302, doi: 10.1021/jp401019p, 2013.

Jena, K. C. and Hore, D. K.: Variation of Ionic Strength Reveals the Interfacial Water Structure at a Charged Mineral Surface, J. Phys. Chem. C, 113, 15364-15372, doi: 10.1021/jp905475m, 2009.

Jena, K. C., Covert, P. A., and Hore, D. K.: The Effect of Salt on the Water Structure at a Charged Solid Surface: Differentiating Second- and Third-order Nonlinear Contributions, J. Phys. Chem. Lett., 2, 1056-1061, doi: 10.1021/jz200251h, 2011.

Karlsson, M., Craven, C., Dove, P. M., and Casey, W. H.: Surface Charge Concentrations on Silica in Different 1.0 M Metal-Chloride Background Electrolytes and Implications for Dissolution Rates, Aquat. Geochem., 7, 13-32, doi: 10.1023/a:1011377400253, 2001.

Kiselev, A., Bachmann, F., Pedevilla, P., Cox, S. J., Michaelides, A., Gerthsen, D., and Leisner, T.: Active sites in heterogeneous ice nucleation—the example of K-rich feldspars, Science, 355, 367-371, doi: 10.1126/science.aai8034, 2017.

Li, Y. and Somorjai, G. A.: Surface Premelting of Ice, J. Phys. Chem. C, 111, 9631-9637, doi: 10.1021/jp071102f, 2007.

Lis, D., Backus, E. H. G., Hunger, J., Parekh, S. H., and Bonn, M.: Liquid flow along a solid surface reversibly alters interfacial chemistry, Science, 344, 1138-1142, doi: 10.1126/science.1253793, 2014.

Lovering, K. A., Bertram, A. K., and Chou, K. C.: Transient Phase of Ice Observed by Sum Frequency Generation at the Water/Mineral Interface During Freezing, J. Phys. Chem. Lett., 8, 871-875, doi: 10.1021/acs.jpclett.6b02920, 2017.

Luca, A. A. T., Hebert, P., Brevet, P. F., and Girault, H. H.: Surface second-harmonic generation at air/solvent and solvent/solvent interfaces, J. Chem. Soc. Faraday Trans., 91, 1763-1768, doi: 10.1039/ft9959101763, 1995.

Lützenkirchen, J. and Behra, P.: On the surface precipitation model for cation sorption at the (hydr)oxide water interface, Aquat. Geochem., 1, 375-397, doi: 10.1007/bf00702740, 1995.

Morag, J., Dishon, M., and Sivan, U.: The Governing Role of Surface Hydration in Ion Specific Adsorption to Silica: An AFM-Based Account of the Hofmeister Universality and Its Reversal, Langmuir, 29, 6317-6322, doi: 10.1021/la400507n, 2013.

Nagata, Y., Hama, T., Backus, E. H. G., Mezger, M., Bonn, D., Bonn, M., and Sazaki, G.: The Surface of Ice under Equilibrium and Nonequilibrium Conditions, Acc. Chem. Res., 52, 1006-1015, doi: 10.1021/acs.accounts.8b00615, 2019.

Ohno, P. E., Saslow, S. A., Wang, H.-f., Geiger, F. M., and Eisenthal, K. B.: Phase-referenced nonlinear spectroscopy of the α-quartz/water interface, Nat. Commun., 7, 13587, doi: 10.1038/ncomms13587, 2016.

Ong, S., Zhao, X., and Eisenthal, K. B.: Polarization of water molecules at a charged interface: second harmonic studies of the silica/water interface, Chem. Phys. Lett., 191, 327-335, doi: 10.1016/0009-2614(92)85309-X, 1992.

Ostroverkhov, V., Waychunas, G. A., and Shen, Y. R.: Vibrational spectra of water at water/α-quartz (0 0 0 1) interface, Chem. Phys. Lett., 386, 144-148, doi: 10.1016/j.cplett.2004.01.047, 2004.

Ostroverkhov, V., Waychunas, G. A., and Shen, Y. R.: New Information on Water Interfacial Structure Revealed by Phase-Sensitive Surface Spectroscopy, Phys. Rev. Lett., 94, 046102, doi: 10.1103/PhysRevLett.94.046102, 2005.

Parambil, J. V., Poornachary, S. K., Tan, R. B. H., and Heng, J. Y. Y.: Template-induced polymorphic selectivity: the effects of surface chemistry and solute concentration on carbamazepine crystallisation, CrystEngComm, 16, 4927-4930, doi: 10.1039/c3ce42622j, 2014.

Rao, Y., Tao, Y.-s., and Wang, H.-f.: Quantitative analysis of orientational order in the molecular monolayer by surface second harmonic generation, J. Chem. Phys., 119, 5226-5236, doi: 10.1063/1.1597195, 2003.

Rehl, B., Rashwan, M., DeWalt-Kerian, E. L., Jarisz, T. A., Darlington, A. M., Hore, D. K., and Gibbs, J. M.: New Insights into χ(3) Measurements: Comparing Nonresonant Second Harmonic Generation and Resonant Sum Frequency Generation at the Silica/Aqueous Electrolyte Interface, J. Phys. Chem. C, 123, 10991-11000, doi: 10.1021/acs.jpcc.9b01300, 2019.

Rosenberg, R.: Why Is Ice Slippery?, Phy. Today, 5, 50-55, doi: 10.1063/1.2169444, 2005.

Schaefer, J., Gonella, G., Bonn, M., and Backus, E. H. G.: Surface-specific vibrational spectroscopy of the water/silica interface: screening and interference, Phys. Chem. Chem. Phys., 19, 16875-16880, doi: 10.1039/c7cp02251d, 2017.

Schaefer, J., Backus, E. H. G., and Bonn, M.: Evidence for auto-catalytic mineral dissolution from surface-specific vibrational spectroscopy, Nat. Commun., 9, 3316, doi: 10.1038/s41467-018-05762-9, 2018.

Schrader, A. M., Monroe, J. I., Sheil, R., Dobbs, H. A., Keller, T. J., Li, Y., Jain, S., Shell, M. S., Israelachvili, J. N., and Han, S.: Surface chemical heterogeneity modulates silica surface hydration, Proc. Natl. Acad. Sci. U.S.A., 115, 2890-2895, doi: 10.1073/pnas.1722263115, 2018.

Seidel, A., Löbbus, M., Vogelsberger, W., and Sonnefeld, J.: The kinetics of dissolution of silica 'Monospher' into water at different concentrations of background electrolyte, Solid State Ion., 101-103, 713-719, doi: https://doi.org/10.1016/S0167-2738(97)00289-0, 1997.

Shen, Y. R.: Optical Second Harmonic Generation at Interfaces, Annu. Rev. Phys. Chem., 40, 327-350, doi: 10.1146/annurev.pc.40.100189.001551, 1989.

Sosso, G. C., Chen, J., Cox, S. J., Fitzner, M., Pedevilla, P., Zen, A., and Michaelides, A.: Crystal Nucleation in Liquids: Open Questions and Future Challenges in Molecular Dynamics Simulations, Chem. Rev., 116, 7078-7116, doi: 10.1021/acs.chemrev.5b00744, 2016.

Steiner, A. L., Mermelstein, D., Cheng, S. J., Twine, T. E., and Oliphant, A.: Observed Impact of Atmospheric Aerosols on the Surface Energy Budget, Earth Interact., 17, 1-22, doi: 10.1175/2013ei000523.1, 2013.

Wang, B., Knopf, D. A., China, S., Arey, B. W., Harder, T. H., Gilles, M. K., and Laskin, A.: Direct observation of ice nucleation events on individual atmospheric particles, Phys. Chem. Chem. Phys., 18, 29721-29731, doi: 10.1039/c6cp05253c, 2016.

Whale, T. F., Holden, M. A., Wilson, Theodore W., O'Sullivan, D., and Murray, B. J.: The enhancement and suppression of immersion mode heterogeneous ice-nucleation by solutes, Chem. Sci., 9, 4142-4151, doi: 10.1039/c7sc05421a, 2018.

Yang, Z., Bertram, A. K., and Chou, K. C.: Why Do Sulfuric Acid Coatings Influence the Ice Nucleation Properties of Mineral Dust Particles in the Atmosphere?, J. Phys. Chem. Lett., 2, 1232-1236, doi: 10.1021/jz2003342, 2011.

Zhao, X., Ong, S., and Eisenthal, K. B.: Polarization of water molecules at a charged interface. Second harmonic studies of charged monolayers at the air/water interface, Chem. Phys. Lett., 202, 513-520, doi: 10.1016/0009-2614(93)90041-X, 1993.

Zhuang, X., Miranda, P. B., Kim, D., and Shen, Y. R.: Mapping Molecular Orientation and Conformation at Interfaces by Surface Nonlinear Optics, Phys. Rev. B, 59, 12632-12640, doi: 10.1103/PhysRevB.59.12632, 1999.

Zipori, A., Reicher, N., Erel, Y., Rosenfeld, D., Sandler, A., Knopf, D. A., and Rudich, Y.: The Role of Secondary Ice Processes in Midlatitude Continental Clouds, J. Geophys. Res. Atmos., 123, 12762-12777, doi: 10.1029/2018jd029146, 2018.

Zobrist, B., Marcolli, C., Peter, T., and Koop, T.: Heterogeneous Ice Nucleation in Aqueous Solutions: the Role of Water Activity, J. Phys. Chem. A, 112, 3965-3975, doi: 10.1021/jp7112208, 2008.

Zumdahl, S. S.: Chemistry, 3 ed., D C Heath Canada, 1123 pp., 1993.

IV. Revised SI with tracked changes

Supporting information (SI) for:

Cloud history can change~~s~~ water-ice-surface interactions of oxide mineral aerosols ~~(e.g. Silica)~~: a case study on silica

Ahmed Abdelmonem[1*], Sanduni Ratnayake[2], Jonathan D. Toner[3] and Johannes Lützenkirchen[2]

[1]Institute of Meteorology and Climate Research - Atmospheric Aerosol Research (IMKAAF), Karlsruhe Institute of Technology (KIT), 76344 Eggenstein-Leopoldshafen, Germany
[2]Institute of Nuclear Waste Disposal (INE), Karlsruhe Institute of Technology (KIT), 76344 Eggenstein-Leopoldshafen, Germany
[3]Department of Earth & Space Sciences, University of Washington, Seattle, WA 98195, USA
* Correspondence to: A. Abdelmonem (ahmed.abdelmonem@kit.edu)

SI1 Thermodynamic considerations

Calculations have been done using and data pertaining to silica (Marion et al., 2009) combined with the the frezchem database included in PHREEQC Interactive, version 3.4.0.12927 (released November 9, 2017). The calculations were done for the experimental conditions at room temperature in terms of solution composition. Two extreme cases were considered: Ice formation and no ice formation. When including the formation of ice, super-cooling cannot be simulated. In this case the pH drops in the H_2O fraction that is not freezing because the solutes are concentrated in ~~remaining~~ liquid that remains due to the freezing point depression. Since in the experiments in no case all of the water freezes, the calculations overestimate the effect. The final calculated volume of liquid water at -40 °C is about 300 µL, which contains all the solutes. In this case the pH drops to about -1.4. In our experiments, the freezing and melting is occurring at the surface. So extreme conditions could occur during the melting only, when remaining solution connects to the interfacial water film, but as pointed out above in all cycles much larger volumes of liquid water are expected compared to the 300 µL noted above. The amount of dissolved silica as a function of the temperature at equilibrium is shown in Figure S1 as a dotted line. The equilibrium concentration of silica at -40°C is about 100 µM based on the available thermodynamic data.

When excluding the formation of ice in the calculation as the other extreme, the water remains liquid and slightly changes its volume, which affects molar concentrations accordingly. The pH remains more or less constant in this case. The concentration of silica at -40°C is about 410 µM, i.e. a factor 4 higher than in the previous case. This is due to the higher salt concentration in the previous example, where the activity coefficients of the solutes cause a decrease in the solubility.

The measured concentration of silica in the experiments was about 41 µM.

The measurements and observations can be related to the above calculations as follows:

- The measured silica concentration (at the end of the experiment at TP cycle 25) is below any of the estimates for equilibrium solubility for the conditions of our experiments. This means that there is a driving force for further dissolution. This corroborates that the number of cycles is the major factor and not the time of exposure, since the prolonged time of exposure at room temperature (i.e. TP > 25) should have caused more dissolution and thus more SHG enhancement. Instead the freeze/melt cycles cause the changes in SHG ~~since~~ with lowering temperature.
- The lower silica solubility, with decreasing temperature, should favor the interaction of dissolved silica with the fused silica surface. Based on the work by (Schaefer et al., 2018), this corroborates the idea that there is a trend to silica adsorption with the decreased temperature. There is ample information for example that dissolved Al adsorbs to aluminium oxide and our experiments with dissolved silica in the presence of fused silica also shows such interaction, so that the temperature dependence in terms of silica solubility would corroborate our interpretation in the main text.

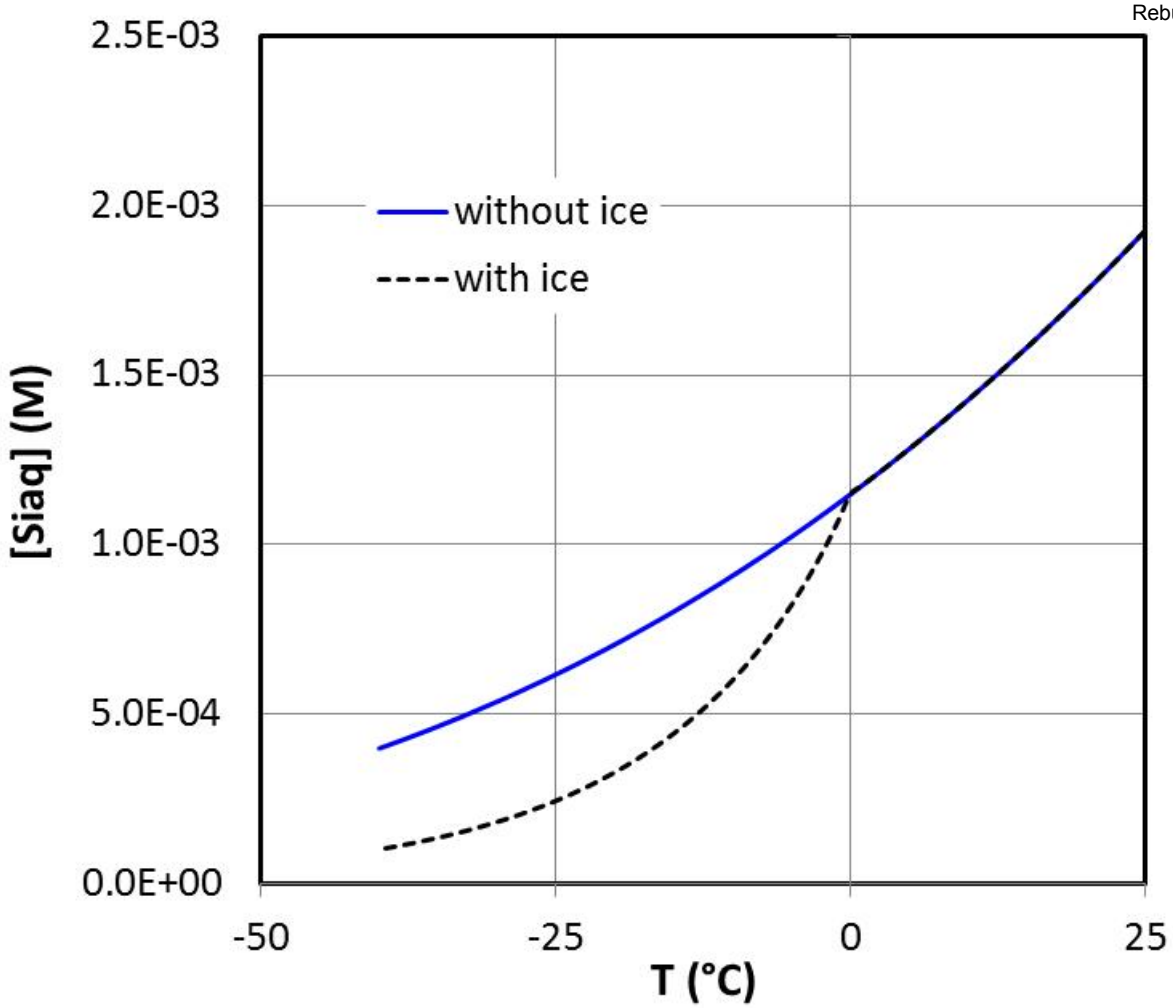

Figure S1: Evolution of dissolved silica in a solution of 1 mM HCl (pH 3 at room temperature) with decreasing temperature in the presence of ice formation (dotted line) and without ice forming (full line). Calculations were done as specified in the text.

SI2 Comparison between PM and SM polarization combinations under the geometrical conditions of the used SHG setup

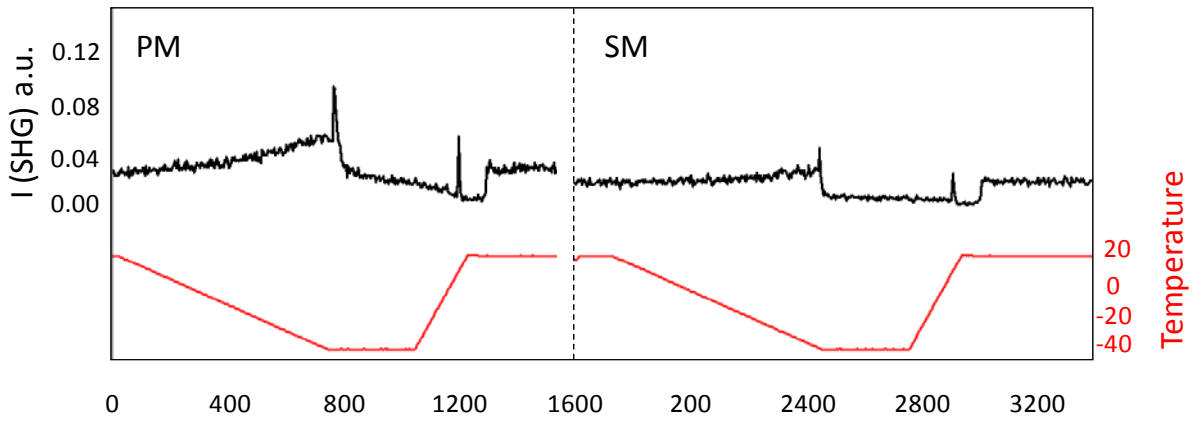

Figure S2: SHG signal (rescaled raw data) at the aged pH3 solution-silica interface as a function of time/temperature for two successive TP cycles with different beam polarization combinations (PM: P-polarized SHG / 45°-polarized incident, and SM: S-polarized SHG / 45°-polarized incident) incident with an angle close to the critical angle of total internal reflection. An aged sample was used to minimize the sample surface change during the two runs. The data show that the signal versus temperature for both polarization combinations behaves identically.

SI3 SHG vs. Cycle number during cooling at different temperatures

Fig 4c in the manuscript looks identical to 4b. It is our intention to show that at the onset point, Fig 4c, there is nothing exceptional happens although the onset temperatures are different.

In Fig. S3 we show the change in signal with aging at other temperatures. Since the paper discusses the restructuring of water upon cooling and relates this to the freezing process, we select here a set of temperatures during cooling to plot the signal as a function of cycle number. Figure S3 shows the averaged SHG liquid signal as a function of TP cycle number at five different temperatures on the cooling path. The minimum points occur at lower cycle numbers for lower temperatures (summarized in table S1). The closest cycle number to the liquid signal minimum decreases with temperature. This assists our conclusion that cooling favors the uptake of dissolved silica (i.e. adsorption).

Time with respect to scan start (s)	Temperature (°C)	Closest cycle no. to minimum signal
a) 0 sec	20	7
b) 120 sec	10	6
c) 240 sec	0	5
d) 480 sec	-20	4
e) 630 sec	-32	3

Table S1: The selected temperatures in Figure S3 and the corresponding TP cycle number of minimum SHG liquid signal.

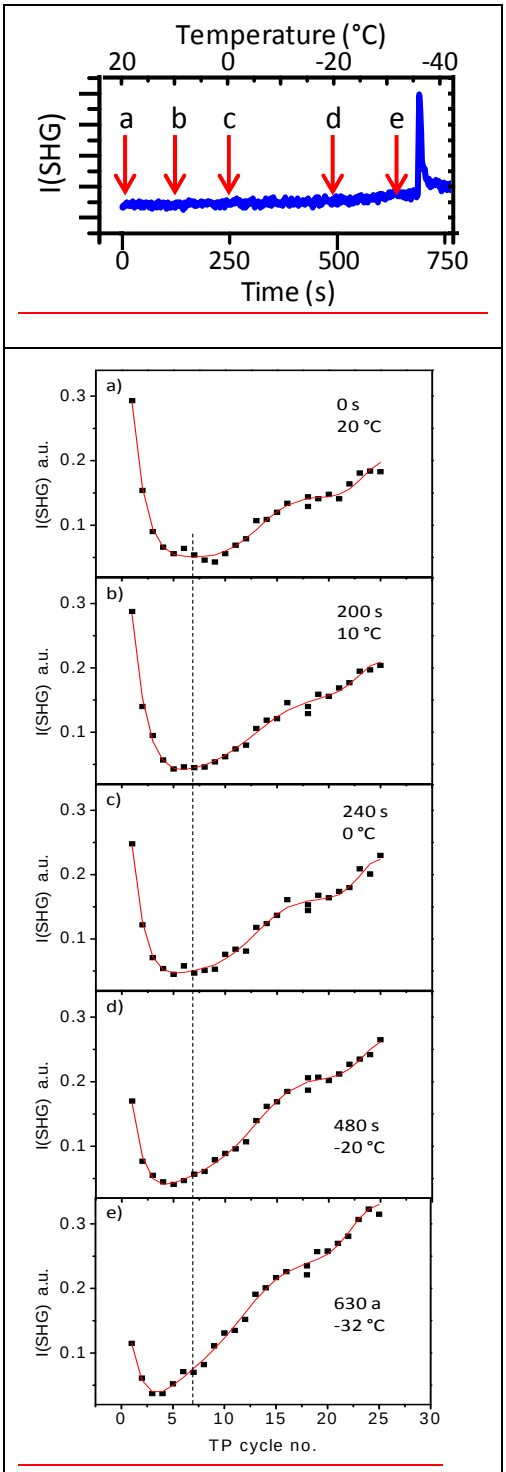

Figure S3: Upper panel: a sample plot of SHG vs. cycle number during cooling. Lower panel: The averaged SHG liquid signal as a function of TP cycle number at five different temperatures during cooling before freezing. The red lines on the plots are guiding lines through the data points.

SI~~3~~4 The observed fast aging, is it a matter of time only?

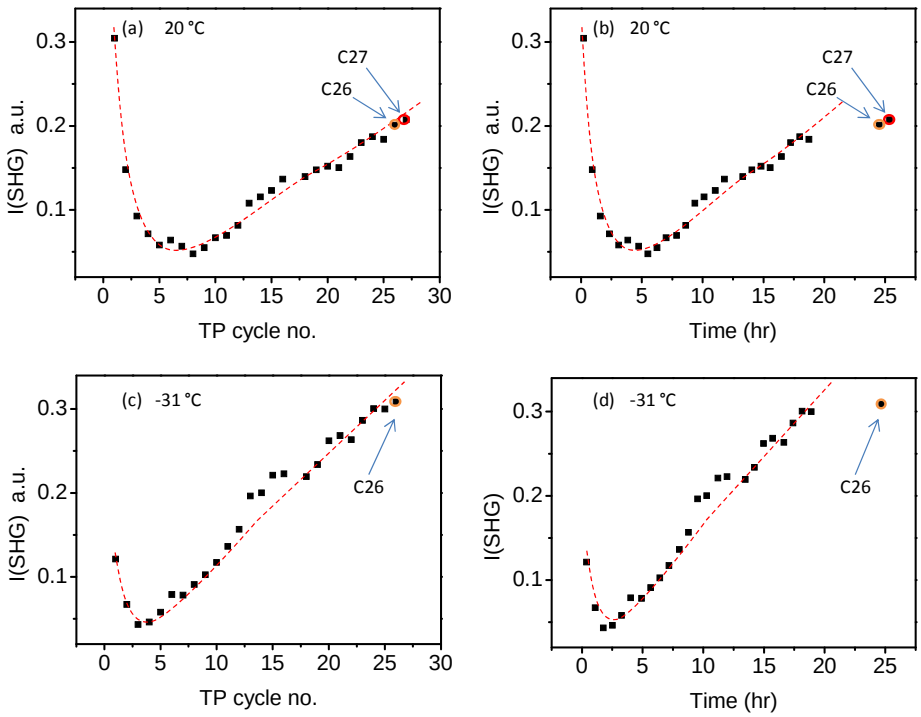

Figure S~~3~~4: SHG signal at pH3 solution-silica interface as a function of TP cycle number (a) and time (b) of liquid signal at 20 °C during repeating the freezing-melting TP. The dashed red lines are trend lines. CS26 and CS27 denote data points that lie on the trend line in (a) but not in (b). This shows that the significant aging we observe in this work arises from the freezing-melting process and not from the time the sample being in contact with solution. Furthermore, as discussed in section S1, the measured silica concentration should favor further dissolution at room temperature, but this does not explain the SHG data.

SI45 SHG versus pH for our Si sample used in this work

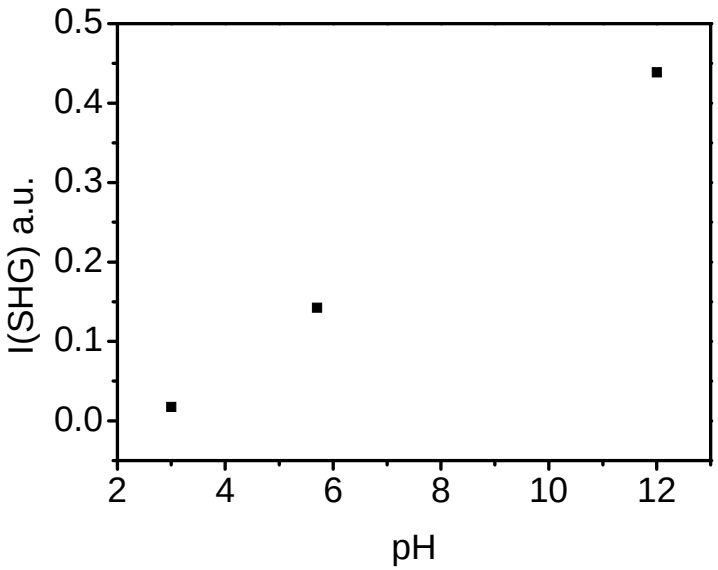

Figure S45: SHG signal as a function of pH for our fresh sample (before aging) at 20 °C.

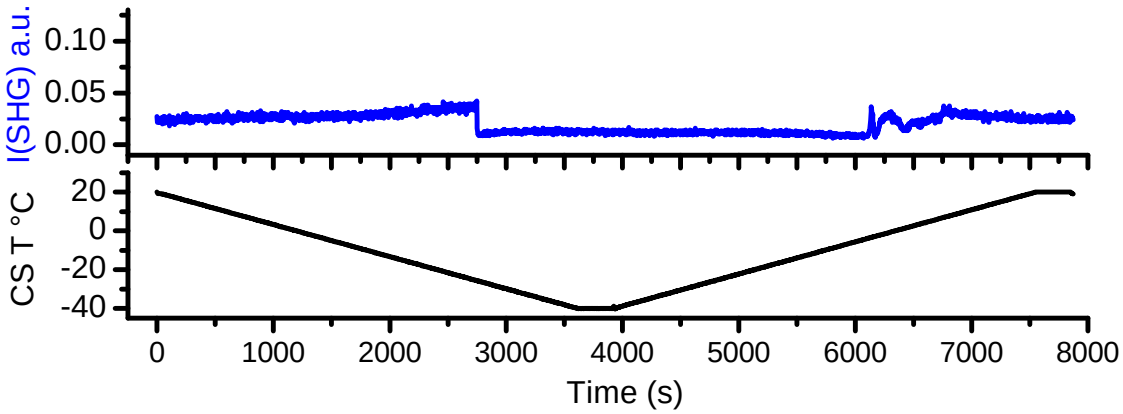

Figure S~~5~~6: SHG signal at pH3 solution-silica interface as a function of time for the C27 run which was carried out at cooling and heating rates (= 1 °C / min) slower than the standard TP.

SI67 Top view of the measuring cell with partially frozen water

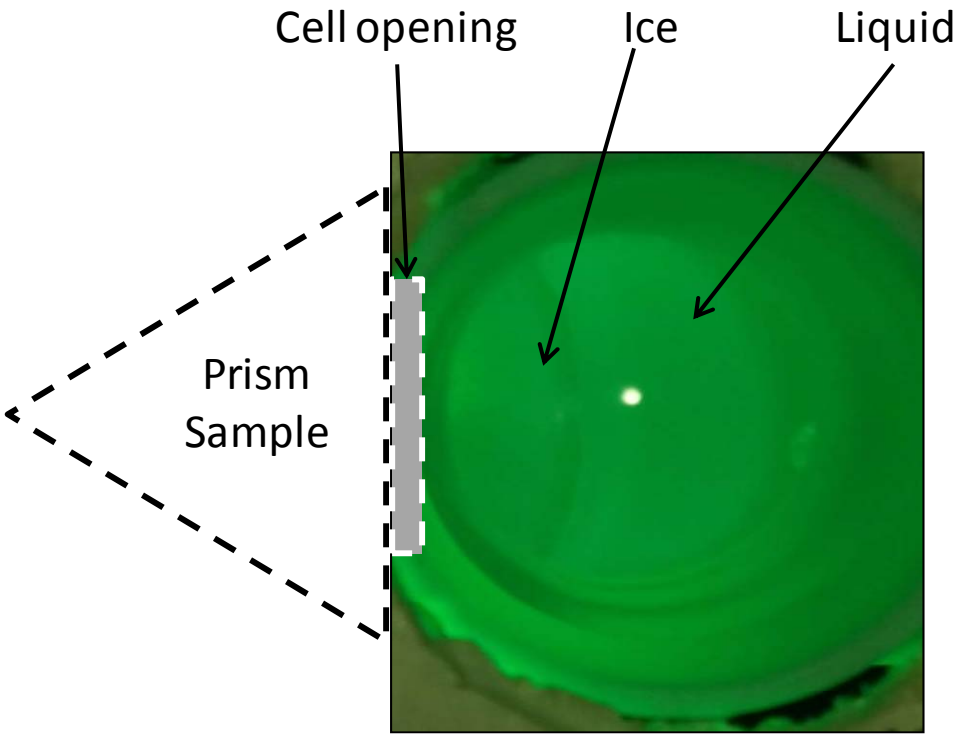

Figure S67: Photo (top view) of the bulk ice formed after freezing and waiting for 5 min at -40 °C. The freezing starts at the surface of the sample and grows at the expense of water on the other side. The size of the bulk ice is proportional to the time of keeping the system supercooled after the freezing event. The ice piece is stuck in the cell opening and the process of melting and departing from the sample neighborhood depends on the cell geometry and bulk ice size as well as the thermal conditions. All these parameters affect the appearance and disappearance of the confined liquid signal.

References

Marion, G. M., Crowley, J. K., Thomson, B. J., Kargel, J. S., Bridges, N. T., Hook, S. J., Baldridge, A., Brown, A. J., Ribeiro da Luz, B., and de Souza Filho, C. R.: Modeling aluminum–silicon chemistries and application to Australian acidic playa lakes as analogues for Mars, Geochimica et Cosmochimica Acta, 73, 3493-3511, doi: https://doi.org/10.1016/j.gca.2009.03.013, 2009.

Schaefer, J., Backus, E. H. G., and Bonn, M.: Evidence for auto-catalytic mineral dissolution from surface-specific vibrational spectroscopy, Nat. Commun., 9, 3316, doi: 10.1038/s41467-018-05762-9, 2018.